

# SOLAR ACTIVITY AND THE CORONA

(*Invited Review*)

B. C. LOW

*High Altitude Observatory, National Center for Atmospheric Research\*, Boulder,  
CO 80307-3000, U.S.A.*

(Received 20 November, 1995; in revised form 5 February, 1996)

**Abstract.** This review puts together what we have learned about coronal structures and phenomenology to synthesize a physical picture of the corona as a voluminous, thermally and electrically highly-conducting atmosphere responding dynamically to the injection of magnetic flux from below. The synthesis describes complementary roles played by the magnetic heating of the corona, the different types of flares, and the coronal mass ejections as physical processes by which magnetic flux and helicity make their way from below the photosphere into the corona, and, ultimately, into interplanetary space. In these processes, a physically meaningful interplay among dissipative magnetohydrodynamic turbulence, ideal ordered flows, and magnetic helicity determines how and when the rich variety of relatively long-lived coronal structures, spawned by the emerged magnetic flux, will evolve quasi-steadily or erupt with the impressive energies characteristic of flares and coronal mass ejections. Central to this picture is the suggestion, based on recent theoretical and observational works, that the emerged flux may take the form of a twisted flux rope residing principally in the corona. Such a flux rope is identified with the low-density cavity at the base of a coronal helmet, often but not always encasing a quiescent prominence. The flux rope may either be bodily transported into the corona from below the photosphere, or reform out of a state of flaring turbulence under some suitable constraint of magnetic-helicity conservation. The appeal of this synthesis is its physical simplicity and the manner it relates a large set of diverse phenomena into a self-consistent whole. The implications of this view point are discussed.

The topics covered are: the large-scale corona; helmet streamers; quiescent prominences; coronal mass ejections; flares and heating; magnetic reconnection and magnetic helicity; and, the hydromagnetics of magnetic flux emergence.

## 1. Introduction

To quote E. N. Parker, if it were not for its variable magnetic field, the Sun would have been a rather uninteresting star. New magnetic fields continually well up into the solar atmosphere as the result of dynamo action in the solar interior (Gilman, 1986; Parker, 1979, 1987; Priest, 1982; Zirin, 1988). The rich collection of radiative, plasma, and MHD phenomena we call solar activity all arise from these magnetic fields making their tortuous way through the different layers of the solar atmosphere and into interplanetary space. This global process proceeds in cycles of approximately eleven years. Instead of ending up in a completely chaotic mix, each cycle of new fields wipes out a pre-existing dipolar global field within a year or two from the beginning of the cycle and replaces it with another

\* The National Center for Atmospheric Research is sponsored by the National Science Foundation.

of comparable strength but the opposite sign (Howard, 1972; Wilson, McIntosh, and Snodgrass, 1990). While this appears to be the normal run of activity in the last two centuries, historical records of solar behaviors of earlier times and recent photometric surveys of sun-like stars suggest that the level of solar activity can vary significantly (Radick, Lockwood, and Baliunas, 1990). There were times such as the period of the Maunder Minimum (1645–1715) when activity appears to have almost completely disappeared (Eddy, 1978).

The magnetic field actually involves only a tiny fraction of the outpouring of energy from the solar core, but it produces quite dramatic consequences as seen in the diverse phenomena in the solar atmosphere and in the variability of the Sun's radiative and plasma outputs which have significant impacts on the terrestrial atmosphere (Pap *et al.*, 1994; Shea, 1991). Traditionally solar phenomena have been studied as separate classes, e.g., sunspots, flares, prominences, etc. This is not unreasonable, given the complexity of each of these phenomena and the need to first figure out their physical nature before attempting to relate them. This review takes a different approach and offers a unified view which relates these phenomena directly to the solar atmosphere's response to the cyclical injection of fresh magnetic flux. This synthesis follows up on several recent developments, both observational and theoretical, in the study of the corona as an electrically highly-conducting atmosphere. The freezing of magnetic flux into the huge volume of the corona makes for observable effects of magnetic-flux emergence if we know what to look for physically. In deducing the relationship between the two major products of activity in the corona – flares and coronal mass ejections – we will be taken beyond coronal concerns to say something about the nature of flux emergence at the photosphere as a part of the global process. In particular, a case will be made for the transport of largely disengaged bundles of magnetic flux through the photosphere into the corona to be eventually expelled out into interplanetary space. This review is organized to take the reader through the physics of coronal processes to arrive at this view of magnetic-flux emergence.

## 2. The Large-Scale Corona

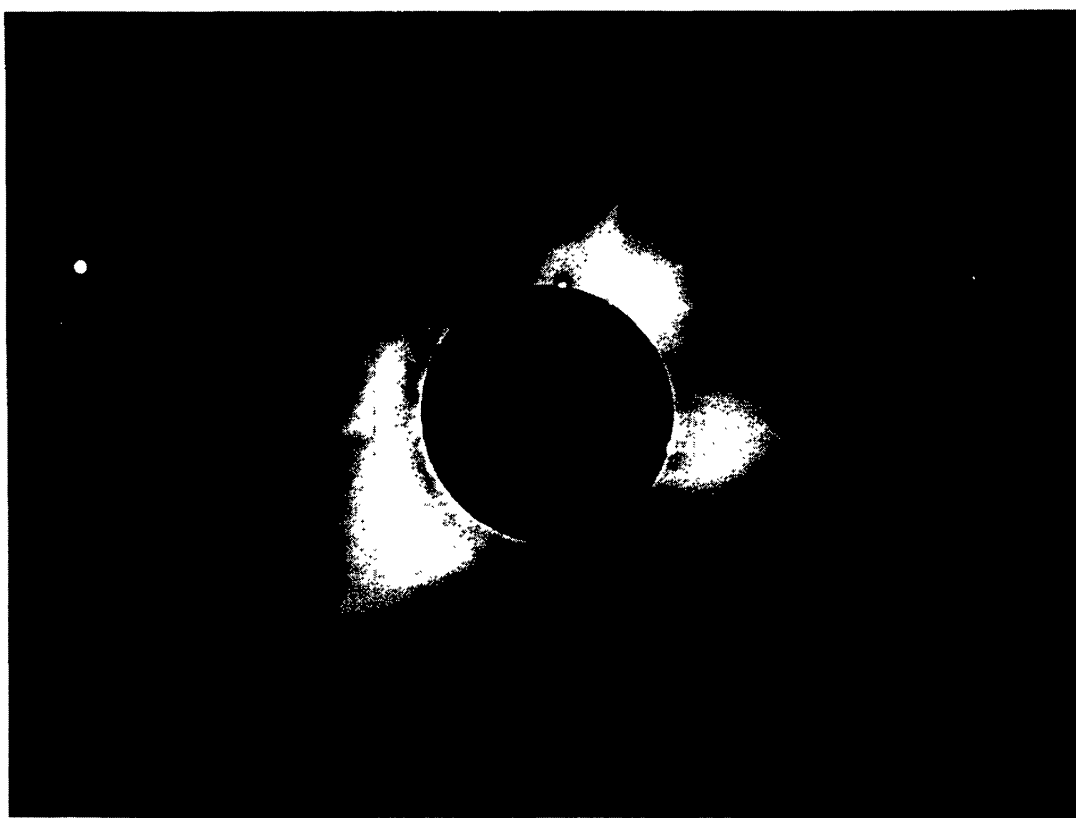
Heating keeps the temperature of the corona in the million-degree range. The precise mechanisms operating are still being debated (Cargill, 1993; Habbal, 1992; Hollweg, 1991; Parker, 1979, 1988, 1994a; Zirker, 1993). For the purpose of this review, we will take the million-degree temperature as given and refer the reader to the references cited for the different points of view on heating. We will see in this section that the high coronal temperature plays a central role in the large-scale ordering of the quiescent corona and its eruption.

## 2.1. THE QUIESCENT CORONA

The thermal conductivity of the corona – a fully-ionized gas at a million-degree temperature – is so efficient that its high temperature extends out to a great distance from the Sun (Parker, 1963). This is the reason for the distended form of the corona in classical eclipse photographs such as the one in Figure 1(a). The hydrostatic density scale-height is about a tenth of the solar radius in the low corona and increases unboundedly with heliocentric radial distance further out, since solar gravity drops rapidly in inverse proportion to the radial distance squared. Combined with the high temperature, the pressure of the distended corona cannot be confined by gravity outside of about  $3 R_{\odot}$  in heliocentric distance. In this outer corona, the atmosphere expands freely into interplanetary space as the supersonic solar wind (Hundhausen, 1972; Parker, 1963).

The expansion of the corona is complicated by the presence of the magnetic field (e.g., Heinemann and Olbert, 1978; Hu and Low, 1989; Pneuman and Kopp, 1971; Sakurai, 1985; Steinolfson, Suess, and Wu, 1982; Tsinganos and Low, 1989). At the million-degree temperature, the electrical conductivity in the corona is so large that for all observable scales (i.e.,  $> 10^3$  km) the corona may be taken for most purposes to be a perfect electrical conductor, with a frozen-in field (Parker, 1979). The Lorentz force exerted by the magnetic field can be decomposed into a pressure gradient force and a tension force. The magnetic pressure enhances the coronal plasma's tendency to expand outward. However, the magnetic tension force may counter the outward expansion if it acts sunward. This is possible under two conditions: if the field is strong enough to dominate over the plasma, and, if it is closed with the two ends of the lines of force anchored to the base of the corona. These conditions are met low in the corona over a photospheric polarity-inversion line, where pockets of dense plasma in the form of helmet like structures are trapped in static equilibrium. Outside of these trapped plasmas, the magnetic field is open, along which the solar wind flows into interplanetary space. The large-scale quiescent corona is therefore structured by the competition between two opposing effects, namely, the general tendency of the hot corona to expand into the solar wind and the opposing tendency of anchored bipolar magnetic fields to seek a closed configuration in which plasma may be trapped under the condition of high electrical conductivity. Based on this consideration, the magnetic field of the corona in Figure 1(a) may be interpreted to be as sketched in Figure 1(b), showing the corona in a dichotomy of two distinct dynamical states, characterized by closed and open magnetic topologies (Hundhausen, 1977, 1994).

The extensive regions of open magnetic fields over the poles are identified with the coronal holes, discovered in the 1970s and subsequently found to be the sources of the high-speed solar winds observed at Earth orbit (Zirker, 1977). It is principally this observational success which lends confidence to the interpretation of the large-scale coronal magnetic field sketched in Figure 1(b). This is an important point,



1966 SOLAR ECLIPSE

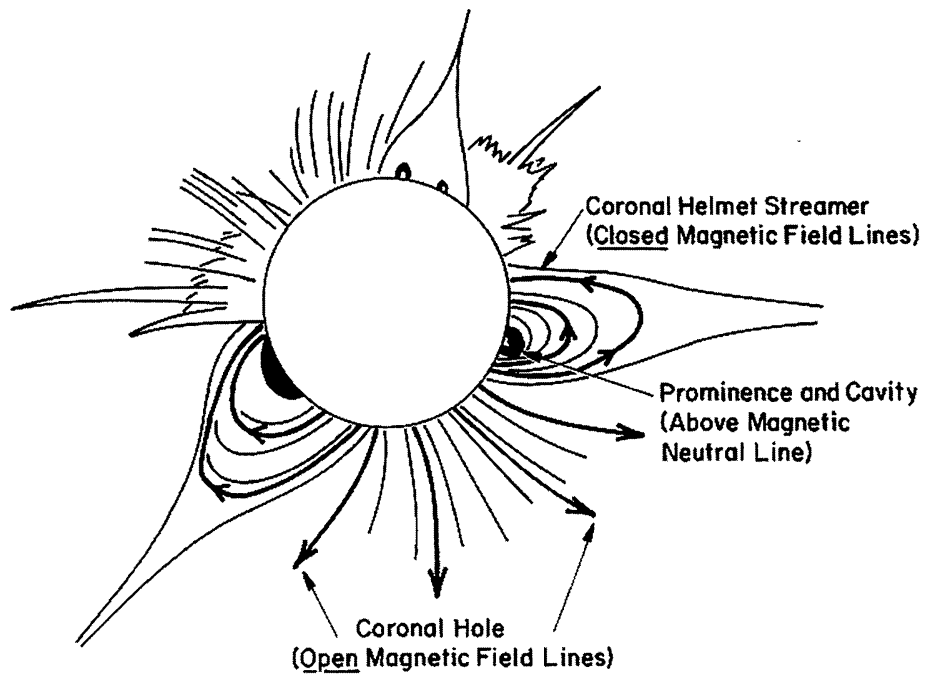


Figure 1. Photograph of the 1974 total eclipse showing the white-light corona with a sketch of the large-scale coronal magnetic lines of force taken from Hundhausen (1994). The lines of force in the coronal holes have one end anchored to the Sun and the other open into interplanetary space. The lines of force in the bright helmet structures are closed with both ends anchored to the Sun.

for the magnetic field in the corona cannot be measured directly with the necessary spatial resolution to map out its global topology.

Two other physical points need to be emphasized in this simple picture of the corona. In both the closed and open field regions low in the corona, say, within  $3 R_{\odot}$  in heliocentric distance, the corona is in approximate magnetostatic equilibrium. The plasma in the closed field regions is static by virtue of magnetic confinement. Although there is a net outward flow in the open-field regions feeding into the solar wind, these regions are approximately static low in the corona where the flow speeds are way subsonic and therefore negligible (Parker, 1963).

The other point concerns the relative strengths of plasma and magnetic forces. At the photosphere, the ratio of the plasma to magnetic pressures, the parameter  $\beta$ , is of order unity. The equal importance of fluid and magnetic forces at this level of the atmosphere is exemplified by the capability of the photospheric plasma to confine the kilo-gauss field of elemental flux tubes and sunspots (Thomas and Weiss, 1991). The photospheric and chromospheric hydrostatic density scale-heights are of the order of 150 km at temperatures of  $5 \times 10^3$ – $10^4$  K. The rapid decline of pressure with height in these thin atmospheric layers compared with the more gradual decline of magnetic pressure (due to flux divergence) results in  $\beta \ll 1$  in the low corona. This is the basis of the popular low- $\beta$  approximation which neglects the plasma pressure and takes the quiescent magnetic fields in the low corona to be force-free, described by

$$\nabla \times \mathbf{B} = \alpha \mathbf{B}, \quad (1)$$

$$\nabla \cdot \mathbf{B} = 0, \quad (2)$$

where the electric current density is set proportional to the magnetic field  $\mathbf{B}$  with proportionality  $\alpha$  (Gold, 1964; Low, 1982a; Low and Lou, 1990; Metcalf *et al.*, 1995; Parker, 1979; Sakurai, 1989). But, over the large scales, of the dimension of a solar radius, this low- $\beta$  approximation is not uniformly valid. In the million-degree environment of the corona, the hydrostatic density scale-height is large, as we have mentioned. The plasma pressure declines with heliocentric distance more slowly over this scale height than the decline of the magnetic pressure due to flux divergence. A comparison of the decline of a isothermal, purely hydrostatic pressure, in the inverse-square gravitational field, of the Sun with that of the magnetic pressure due to a dipole potential magnetic field readily illustrates this point. Hence, although the plasma  $\beta$  is generally small in the low corona, it increases in value with increasing heliocentric distances to order unity where the plasma dominates. Therefore, for the description of the large-scale corona out to where the wind is important, Equation (1) needs to be replaced by

$$\frac{1}{4\pi} (\nabla \times \mathbf{B}) \times \mathbf{B} - \nabla p - \frac{\rho GM_{\odot}}{r^2} \hat{r} = 0, \quad (3)$$

allowing for the forces due to pressure and gravity in the usual notation (Hundhausen, Hundhausen, and Zweibel, 1981; Uchida and Low, 1982; Low and Smith, 1993). The expansion of the corona into the solar wind drags all magnetic fields beyond this region into the open configuration. It should be noted that gravity also plays an important role in the dynamics of the steady solar wind (Parker, 1963). So it is important to bear in mind that plasma pressure, magnetic field, and gravity are all significant agents in the structuring of the large-scale corona.

## 2.2. HELMET STREAMERS

The eclipse picture in Figure 1(a) registers white light Thomson-scattered into the line of sight. Brightness in this picture is proportional to the line-of-sight integral of the electron density, with a weighting favoring the electrons in and near the plane of the solar limb (Billings, 1966; Hundhausen, 1993). Under the assumption of charge neutrality, the white-light brightness is approximately proportional to the mass of the coronal structures at the solar limb. From this consideration, the total mass in a typical helmet structure may be estimated to be in excess of  $10^{15}$  g (Illing and Hundhausen, 1986). This is consistent with a density of a few times  $10^8$  proton cm $^{-3}$  at  $1.5 R_{\odot}$  in heliocentric distance, about an order of magnitude larger than the density in the open-field regions at the same coronal height.

The high density and temperature in the helmet structure can be qualitatively understood in terms of the interplay between force equilibrium and energy balance in a closed magnetic field (Pneuman, 1972). Two important factors influence energy balance in such a magnetic field: (i) the corona is a poor radiator because of its tenuous, fully ionized state, and (ii) thermal conduction is very effectively channelled along the magnetic field. Subject to ubiquitous heating, the plasma in the closed magnetic field has only one way to achieve thermal balance between heat input and loss, which is to have its temperature rise to a level when its thermal radiation and the downward-driven thermal conduction (along the closed magnetic field) are able to balance the total heat input. This qualitative conclusion is consistent with recent emission-line observations of the corona suggesting that the hot parts of the corona tend to coincide with helmet streamer belts (Guhathakurta and Fisher, 1994).

In a slowly evolving magnetic field, this thermal-balance process is coupled to the quasi-static adjustment of forces to keep the structure in approximate equilibrium. Along the magnetic field, the adjustment must produce a pure hydrostatic pressure since the Lorentz force has no component in that direction. A higher temperature then implies a larger hydrostatic density scale height and, therefore, an enhanced density in the closed magnetic field. The enhancement results from heated material from the dense atmosphere below rising up along the anchored magnetic field. The enhancement tends to expand and distend the closed magnetic field. Whether the entire structure remains quiescent, even if distended, or breaks

up dynamically depends on the possibility of confining the increased pressure by the Lorentz force.

In any given situation, the physical conditions at the base of the corona, the surrounding open-field environment, field intensity, heating rates, etc., all contribute to determining whether a coronal helmet may remain in quasi-static force and energy balance. For example, with a large enough heating rate, a closed magnetic field will expand quasi-statically and then opens up catastrophically. The shearing displacement of the footpoints of a closed magnetic field may also lead to its opening up (Forbes, 1992; Klimchuk, 1990; Low, 1981, 1986; Mikić and Linker, 1994; Roumeliotis, Sturrock, and Antiochos, 1994; Steinolfson, 1991; Wolfson, 1982, 1995; Wolfson and Low, 1992). We will take up the question of the breakup of helmet streamers later in our discussion. For the present, we know from observation that helmet streamers are present throughout the solar cycle and are truly long-lived prior to breakup, some persisting for a solar rotation or longer.

The helmet streamer is an arcade-like structure running along and over a polarity-inversion line on the photosphere. It has a three-part structure: a high-density shell with the top tapering into the streamer, a low-density cavity at the base, and a quiescent prominence in the cavity (Engvold, 1989; Saito and Hyder, 1968; Saito and Tandberg-Hanssen, 1973). Depending on the orientation of the line of sight with the length of the arcade, this long structure takes different shapes in the optically thin corona. If we happen to look down the arcade, that is when we see the structure with its characteristic helmet shape: bright helmet dome, cavity, and prominence. At activity minimum, the corona is dominated by the Sun's magnetic dipole. A principal polarity-inversion line, often with a meandering geometry, can be traced on the global photosphere and over this line a helmet arcade can be found (Hundhausen, 1977). At solar maximum when the Sun has lost its magnetic dipole, the corona is complex with very many helmet arcades associated with the multipolar global magnetic field; see Figure 2. The interesting point is that despite the complexity of the corona at activity maximum, the helmet structures are similar to the ones found at activity minimum in that they often have the same three-part structure.

The cavity observed during a particular eclipse is about 3% brighter than the coronal background surrounding the helmet structure, and about 20% as bright as the dense region of the helmet (Saito and Hyder, 1968). This is probably typical. There is no unique way of inverting the integration of the density, along the line of sight through the optically-thin corona, to obtain the density in the cavity, but upper-bound estimates suggest that the cavity density is reduced from that in the helmet by a factor not larger than 10. Spectroscopic observations show that the cavity is at coronal temperatures (Engvold, 1989; Tandberg-Hanssen, 1974). Therefore the cavity is heated but is somehow cut off from a mass source to fill it with high-density plasma. Theoretically the cavity must be a region of enhanced magnetic field whose magnetic pressure makes up for the deficit in plasma pressure so as to sustain the cavity from collapse (Low, 1980). If we take the helmet magnetic field

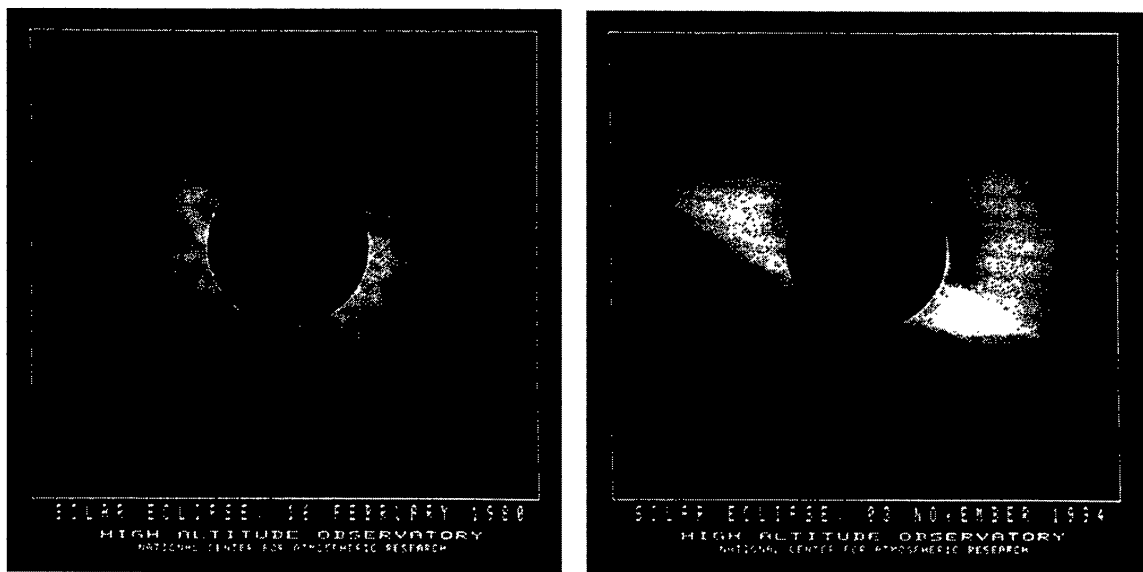


*Figure 2.* The corona in white light during the total eclipses of 1980 (a) and 1994 (b), showing examples of its large-scale configurations at times of activity maximum and minimum, respectively. The minimum-activity corona is dominated by a global dipolar magnetic field which manifests itself as a belt of helmet streamers in the equatorial region. The maximum-activity corona participates in the reversal of the Sun's global magnetic field. In 1980 the dipole magnetic moment is negligible so that the corona is populated with the higher-moment magnetic fields associated with a complex collection of helmet streamer belts, as shown. The eclipse photographs in Figures 1 and 2 belong to the High Altitude Observatory archives.

to be of the order of 10 G, a field increase by a factor of 2 readily can account for the pressure deficit corresponding to the above moderate reduction of density in the cavity. Explaining the density reduction is simple in terms of force-balance requirement. What is difficult to explain is why a part of the helmet magnetic field should be evacuated of plasma.

A quiescent prominence is often, though not always, found in the helmet cavity. This readily suggests that the low density in the cavity may have resulted from a condensation process which produced the prominence. It has long been recognized that this idea is oversimplified, for the observed deficits in cavity mass are too small to account for the masses of the respective prominences (Saito and Hyder, 1968; Saito and Tandberg-Hanssen, 1973). Moreover, it is also known that prominence material tends to drain gradually, requiring replenishment of their plasma over the time scale of a day (Tandberg-Hanssen, 1974). This suggests a more or less steady condensation of material from some source into the prominence during its quiescent state. What we crucially need to know is the form of the magnetic field in the cavity. Direct observational information on the cavity is scarce since it has only weak emissions. On the other hand, indirect information about the cavity magnetic field can be inferred from the observed properties of prominences, if we are prepared to sew the observational results together with a few plausible theoretical ideas. To that purpose, we review the current understanding of the prominence as a plasma object and relate it to its surrounding cavity.

### 2.3. QUIESCENT PROMINENCES

Quiescent prominences, as long-lived condensations typically orders of magnitude cooler ( $10^4$  K) and denser ( $10^{11-12}$  cm $^{-3}$ ) than the surrounding coronal plasmas, are common features over the photospheric polarity-inversion lines throughout the solar cycle (Priest, 1989; Tandberg-Hanssen, 1974, 1995). They are best seen in H $\alpha$  as absorption features, called filaments, against the disk chromosphere or in their own emissions at the limb. Although they can take a variety of complicated shapes and have fine thread-like structures down to the limit of observational spatial resolution, their macroscopic appearance is that of a vertical thin sheet of plasma (width  $\sim 10^4$  km) with a long horizontal dimension ( $\sim 10^5$  km), suspended above the polarity-inversion line.

In very rough terms there are two types of quiescent prominences, those forming in the newly emerged magnetic fields of an active region, and those associated with the decaying phase of an active region (Martin, 1989; Tandberg-Hanssen, 1974, 1995; Tang, 1987; Zirin, 1988). The former are low lying, at heights typically below  $10^4$  km; have the usually curved shapes of their associated inversion lines; and, are more rapidly evolving as to be expected from their active-region environment. The other type of prominences are long-lived and tend to lie over a long and rather straight polarity-inversion line of an aged active region. Such prominences and their polarity inversion lines can be quite long; a length of more than  $1 R_\odot$  is not uncommon. They tend to locate high in the corona, above  $10^4$  km, appearing to rise quasi-statically in height over a half rotation period before they erupt (Hundhausen, 1995a; Zirin, 1988).

Direct measurements reveal that the vector magnetic fields in prominences are predominantly horizontal, pointing within about  $20^\circ$  of the long horizontal axis of the prominence (Leroy, 1989; Leroy, Bommier, and Sahal-Bréchot, 1983, 1984). The horizontal magnetic orientation is consistent with the idea that the prominence is composed of plasma condensations trapped at the lowest points of upward-concave magnetic lines of force under conditions of high electrical conductivity. Such a field topology occurs naturally over a photospheric inversion line. If we take the component of the prominence magnetic field perpendicular to the inversion line, this component tells us whether the magnetic field threads the prominence sheet in a direction the same as or opposite to that of the field linking the bipolar regions on the photosphere below. Combining this topological relationship between the prominence and photospheric magnetic fields, with the fact that a great many prominences are embedded in a cavity under the helmet, we arrive at the two conceptually possible global field topologies for the helmet streamer sketched in Figure 3. In both sketches, a helmet streamer is located over the equator, assumed, for the sake of simplicity, to be axisymmetric about the polar axis and symmetric about the equator. This simple form of the global field is a reasonable approximation of the ‘dipolar’ corona at activity minimum. The arrowed lines are the magnetic lines of force. The open lines of force lie in the meridian plane. The closed lines

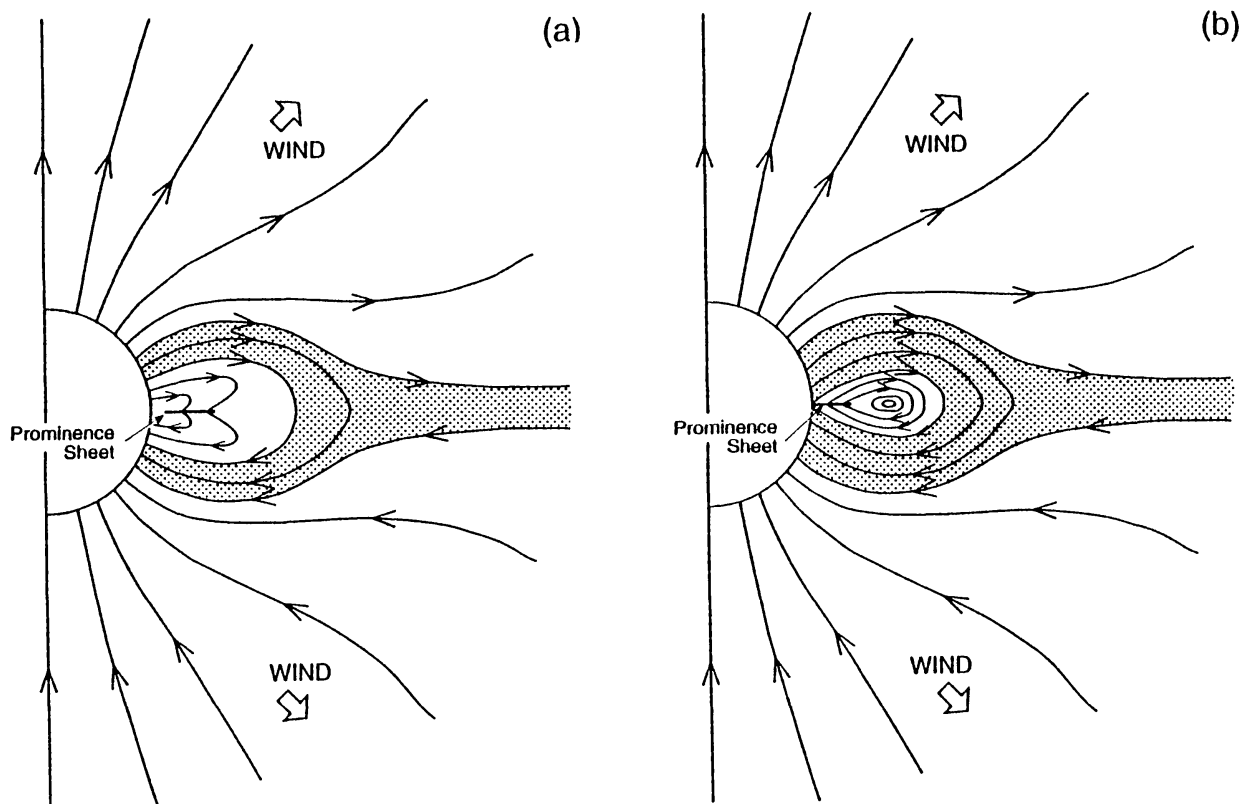


**Figure 3.** Schematic sketches of the helmet streamer with the two basic internal magnetic topologies: normal polarity (a) and inverse polarity (b). In the axisymmetric geometry shown, the arrowed lines indicate magnetic lines of force which are open in the polar regions and closed over the equator. The solar wind escapes along the open lines of force which lie in the meridian plane. The closed magnetic field is in static equilibrium forming the helmet structure. This part of the field carries an azimuthal component so that the arrowed lines shown in the helmet are projections of the lines of force onto the meridian plane. In the helmet structure, the high density dome is shaded in the two cases shown, with a low-density cavity at the base, embedding a vertical prominence sheet, represented as a line, whose length runs in the azimuthal direction. The basic distinction between topologies (a) and (b) is that the closed field in case (b) contains projected lines of force which are detached from the Sun, indicating a flux rope running in the azimuthal direction.

of force are shown as projections in the meridian plane, allowing for a component of the magnetic field in the azimuthal direction, not possible to show explicitly in these figures. The distinction between the two topologies in Figure 3 is that in Figure 3(a), all closed lines of force are in the form of bipolar arches anchored at two ends to the base of the corona, whereas, in Figure 3(b), lines of force closing upon themselves within the corona are also present. Bearing in mind that these lines of forces are seen in projection on the meridian plane and that they carry an azimuthal field component, the field closed within the corona represents a rope of helical flux running above the equator and around the solar axis. The prominence sheet represented by a radial line is threaded by magnetic lines of force which point in the same direction as the surface field in Figure 3(a), and in the opposite direction in Figure 3(b). The prominence configurations in Figures 3(a) and 3(b) are called the normal and inverse configurations (Anzer, 1989; Leroy, 1989).

Two qualifying remarks on Figure 3 will help avoid possible confusion in its interpretation. The first concerns a standard approximation in prominence modeling. Since the prominence is a thin vertical sheet we may neglect its sheet thickness in comparison to the scales of the global corona (Amari, 1990; Anzer, 1989). This approximation is used in Figure 3 where the prominence is shown as a line marking the intersection of the prominence sheet with the meridian plane. This sheet is massive and carries a discrete current flowing in the azimuthal direction. The discrete current is associated with a kink in the magnetic field threading across the prominence sheet, which produces a magnetic tension force to support the weight of the prominence. In Figure 3(a), this support requires the prominence sheet to be suspended in the indented tops of bipolar magnetic arches. In Figure 3(b), one could have also postulated that the prominence sheet is sitting on similarly indented tops of the closed lines of force, but, instead, it is placed at the bottoms of the completely closed flux rope where the upward-concave lines of force naturally give a upward directed magnetic tension force. Intuitively it is clear that the latter is mechanically stable whereas an indentation of a downward-concave line of force is likely to be unstable.

The second remark concerns the physical interpretation of the azimuthal flux rope in Figure 3(b). In the realistic (non-axisymmetric) situation, a flux rope in the corona would likely have finite ends which blend into the complex background fields. What is captured in the axisymmetric idealization in Figure 3(b) is the idea that a realistic magnetic flux rope may levitate with a main part of its length in the corona while the ends of the rope may be anchored to the coronal base in some complicated fashion (e.g., Lites *et al.*, 1995). In contrast to the case of a simple inverted ‘U’ bipolar loop, each of the lines of force of an anchored flux rope rises from one footpoint at the coronal base to wind about the rope axis once or more times within the corona before reaching the other footpoint (Priest, Hood, and Anzer, 1989). In our discussion about the azimuthal flux rope in Figure 3(b), it should always be born in mind that it is a two-dimensional representation of the above more complicated anchored flux rope in realistic situations.

We have shaded the high-density region of the helmets in Figure 3, identifying the unshaded interior around the prominence sheet to be the cavity. As we have pointed out, a moderate increase of the magnetic field intensity, keeping the field geometry unchanged, going from the helmet into the cavity would readily produce a density reduction in both cases. But, on theoretical ground, the normal configuration in Figure 3(a) is artificial in the following sense. It was pointed out earlier that a closed magnetic field, anchored to the dense atmosphere at the coronal base and subject to heating, tends to be filled with dense plasma rising up along the field. This is how the helmet gets its high density. Some additional assumptions must be made if the same process is to be suppressed to produce bipolar fields with reduced densities in a large coherent spatial region. It could be stipulated, of course, that the heating which drives heated plasma to form the high-density dome is absent in the cavity. While its possibility cannot be ruled out *a priori*, such a stipulation is

quite arbitrary and unlikely in view of the fact that the cavity is not significantly cooler than its surrounding (Engvold, 1989; Tandberg-Hanssen, 1974).

On the other hand, a magnetic field closed in the corona like the flux rope in Figure 3(b) would be cut off from the source of plasma at the coronal base since plasma motion across lines of force is negligible by virtue of high electrical conductivity. The thermal shielding of a closed magnetic field would also create the environment for any plasma which does get into the flux rope to rapidly condense to form the prominence (Mason and Bassey, 1983; Poland and Mariska, 1986; Smith and Priest, 1977). In a realistic situation, the cavity is likely to be a flux rope suspended with a main part of its length rather than the entire length in the corona. Although the lines of force may be anchored to the photosphere at two ends, each twisted line of force of the flux rope may be sufficiently tortuous as a path for mass transport and thermal conduction such that the same effect of thermal isolation is produced. Therefore, the presence of a magnetic flux rope can explain not only why the cavity is physically distinct from the high-density region of the helmet but also why a prominence should form in the cavity.

Observations over the years show that the inverse configuration is common whereas the normal configuration is not (Athay *et al.*, 1983; Leroy, 1989; Leroy, Bommier, and Sahal-Bréchot, 1983, 1984). Measured vector magnetic fields show that the majority of crown filaments are of the inverse configuration, with the normal configuration obtaining for a small minority, generally low lying prominences (Athay *et al.*, 1983; Leroy, 1989). These measurements also show a tendency for (i) the magnetic intensity and (ii) the alignment of the magnetic vector with the prominence axis, both to increase with height inside the prominence observed at the limb (House and Smartt, 1982; Leroy, Bommier, and Sahal-Bréchot, 1983; Rust, 1967). These two properties have recently been explained in terms of the magnetic field of a prominence embedded in a flux rope in the inverse configuration (Low, 1993a, Low and Hundhausen, 1995; Schönenfelder and Hood, 1995).

It is not practical to measure the magnetic field of the active region prominences because most of them are located too low in the corona at the limb for direct spectroscopic observation. Unlike the more quiet regions of the solar atmosphere, the chromosphere over an active region is rich with elongated horizontal H $\alpha$  structures interpreted to be nearly horizontal flux tubes of active-region magnetic fields penetrating the chromosphere from below (Foukal, 1971; Zirin, 1988). In the neighborhood of an active-region filament, the swirl and flow of fibrils form a characteristic pattern long recognized by observers. In this pattern, the fibrils have the appearance of streaming parallel to the polarity inversion line above which a filament lies, with no fibrils clearly arching over the inversion line (Foukal, 1971; Martin, Bilimoria, and Tracadas, 1993). The fibrils nearer the inversion line are longer and more aligned with the inversion line. Those farther away are shorter and tend to point away from the inversion line. This characteristic pattern is sketched in Figures 4(a) and 4(b), representing two basic types named sinistral and dextral by Martin, Bilimoria, and Tracadas (1993). For a given pair of bipolar photospheric

regions, if the fibrils on any one side rise into the chromosphere and stream parallel to the inversion line in one direction, the fibrils on the other side rise and stream in the opposite direction.

In contrast, the fibrils associated with an inversion line without a filament are usually observed to arch conspicuously almost at right angle over the inversion line. This is the configuration we would expect of a potential-like bipolar field in an arcade formation. An exception to this observation is the so-called filament channel without a filament which we shall discuss shortly.

The above fibril pattern associated with active-region filaments is not consistent with a prominence in the normal configuration featuring bipolar lines of force arching low over the polarity inversion line. But, it is quite consistent with the idea that the prominence sits in a horizontal magnetic flux rope with the rope axis located in the corona, as sketched in Figure 3(b). The fibrils mark the chromospheric portions of the lines of force originating from the photosphere below. Figure 3(b) shows that no fibrils can arch over the inversion line low in the chromosphere because this region is occupied by the prominence flux rope. The nature of the flux-rope field topology is such that the field is principally axial in the vicinity of the rope axis, but is azimuthal around the rope axis in the outer layer. In Figure 3(b), the fibrils originating near the inversion line, being near the rope axis, have the geometry of the axial field. They are therefore long, horizontal and aligned with the prominence axis. The fibrils away from the inversion line belong to the outer layer of the flux rope. They circulate around the flux rope, and, therefore, rise vertically up the chromosphere. These fibrils (which are the chromospheric part of a line of force) are short, and they also point away from the inversion line in order to make room over the polarity inversion line for the flux rope. Thus, the fibril patterns in Figure 4 are explained, with the two types of pattern related to the two possible signs of the axial field of the flux rope for a fixed sense of the field component circulating around the rope axis. All the fibril morphologies described above have been successfully modeled by explicit solutions to the magnetostatic Equation (3) in both two and three dimensional geometries (Low and Hundhausen, 1995; Lites *et al.*, 1995).

An important point to note is that the characteristic fibril patterns in Figure 4 are related directly to the magnetic flux rope, not necessarily to the presence of the prominence in the flux rope (Low and Hundhausen, 1995). In other words, a flux rope of the type shown in Figure 3(b) without a prominence sheet will have the same basic fibril patterns as shown in Figures 4(a) and 4(b). It has long been recognized that these characteristic fibril pattern can be found in the chromosphere in the absence of a prominence (Martin, 1989; McIntosh, 1972; Serio *et al.*, 1978). Such a lane called a filament channel is independent of the prominence in the sense that while prominences are always found in a channel, the channel may exist without a prominence. Indeed channels may survive several solar rotations with prominences forming, erupting, and reforming within them (Martin, 1989). We may therefore conclude that the common association between filaments and filament

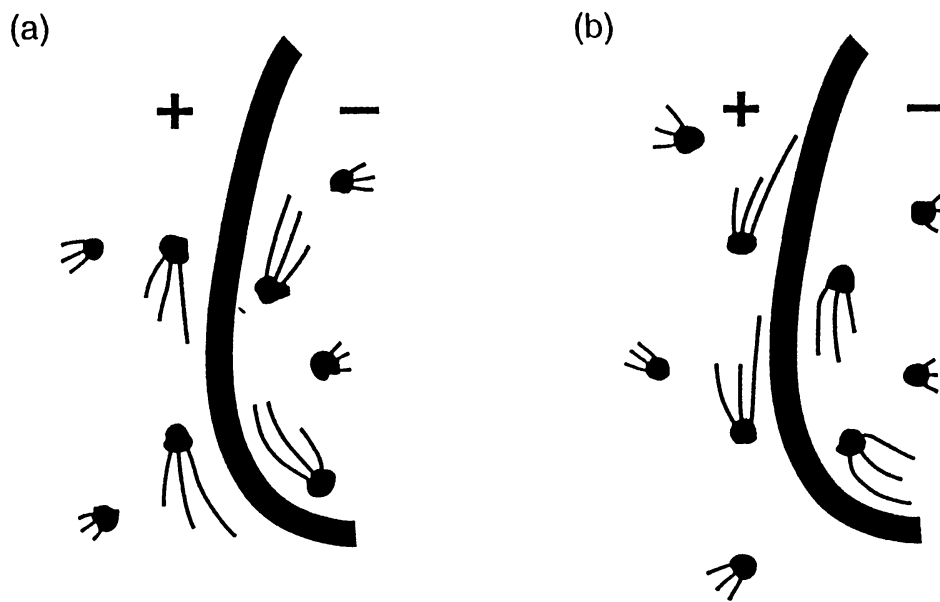


**Figure 4.** Sketches of the observed characteristic fibril pattern in the chromosphere in the neighborhood of an active-region filament, adapted from Martin *et al.* (1993). In the two configurations shown, described by Martin *et al.* as sinistral (a) and dextral (b), the thick long structure represents the filament seen projected on the chromosphere marking the magnetic polarity inversion line. The magnetic polarities of the two regions on the two sides are as indicated. The thin lines represent fibrils, anchored at the chromospheric structures represented as black 'knots', seen in projection, showing long lines near the filament and shorter lines located away from the filament.

channels arises from the favorable thermal environment within the channels for prominence formation whereas the cavity flux ropes giving rise to the channels are fundamental coronal structures quite independent of the prominences.

Martin (1989) has a different interpretation of the inverse configuration in Figure 4 in terms of bipolar field topologies without involving a flux rope. This interpretation deals only with morphological description without justifying the interpretation in terms of a physical model. Antiochos *et al.* (1994) presented yet another interpretation in terms of a model for a three-dimensional, bipolar force-free magnetic field. When a prominence erupts, it is common to observe the flowing prominence material spiraling and outlining helical structures, suggesting that a rope of helical magnetic field embeds the erupted prominence (Tandberg-Hanssen, 1995; Vršnak, Ruždjak, and Rumpolt, 1991). It will be interesting to determine whether the inferred magnetic flux rope is formed at the time of eruption, such as by magnetic reconnection, or has existed before eruption as a part of the global structure. This would be a conclusive way of distinguishing the flux-rope model we favor in this paper from models which do not admit the flux rope as essential to the quiescent prominence in the inverse configuration. In this review we treat Martin's interpretation as separate from her observational results. Our flux-rope model is consistent with the observational results of Martin and others. We will see

in the next two sections that quite independent physical considerations also lead naturally to the flux-rope model.

For a flux rope, the sign of the helicity or handedness of the rope's helical lines of force is related directly to the way the fibrils stream on the two sides of the prominence. In Figure 4, the right- and left-handed helical fields of the flux rope are associated with the dextral and sinistral types, respectively. Martin *et al.* (1993) have concluded that the prominences of the northern and southern hemispheres are predominantly of the dextral and sinistral type, respectively, independent of solar cycle during the past cycles for which data are available; see also Martin and McAllister (1995). This is a fundamental result. That the flux ropes in the same hemisphere, in general, have the same sense of twist, or a fixed handedness, suggests that a global process related to the solar rotation is at work.

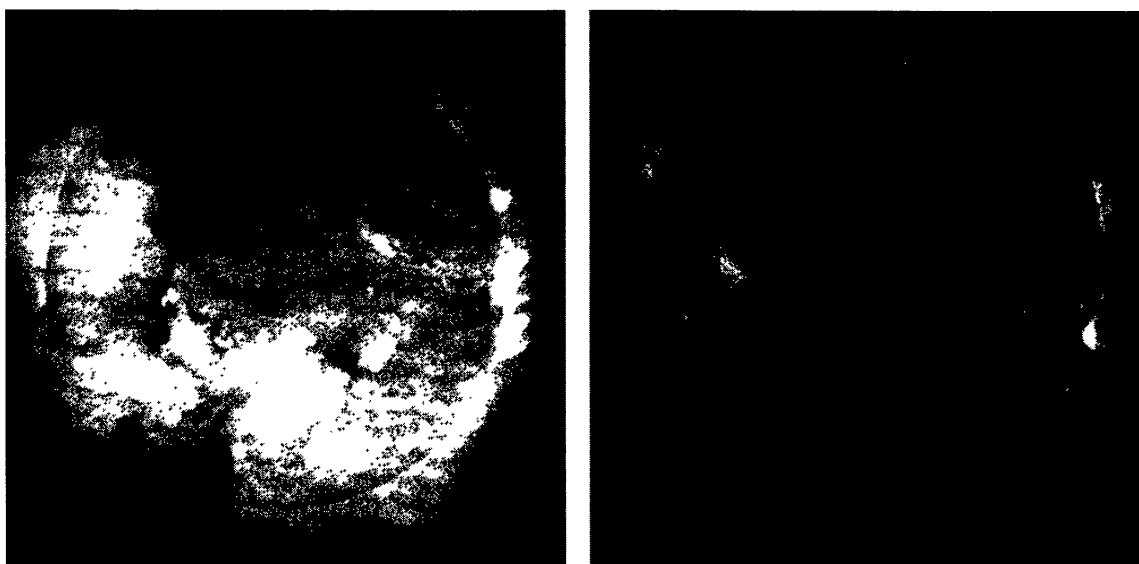
There are several other observations of magnetic twist. The vector magnetic fields measured in the crown filaments have been used to infer the sign of the helicity of the magnetic arcades of the filaments (Leroy, 1989; van Ballegooijen and Martens, 1990). Vector fields measured in active regions give the sign of the twist in the local field through the parameter  $\alpha$  taken as the ratio between the vertical current and the vertical magnetic field (Pevtsov *et al.*, 1994, 1995; Seehafer, 1990). This twist is also in the appearance of fibrils around sunspots (Richardson, 1941). All these other observations corroborate Martin's result on the hemispheric preference for a fixed sign of the helicity independent of solar cycle. The significance of this conclusion will become clear in the next section.

The nature of the magnetic support of the prominence weight in the inverse configuration of Figure 3(b) is also relevant to the next section (Low and Hundhausen, 1995). A detailed analysis of the support problem shows that in this configuration, the prominence sheet is necessarily supported both by the repulsion of the photospheric currents below and by the attraction of the currents above it (Low and Hundhausen, 1995); see also Démoulin and Forbes (1992). The latter currents are those flowing in the largely force-free flux rope of the cavity whose center lies above the prominence sheet; see Figure 3(b). This static force relationship is mutual. It can be restated that the cavity flux rope has a tendency to rise buoyantly into the atmosphere but is anchored, in part, by the weight of the prominence, and, in part, by the weight of the dense helmet with its bipolar field around and above the cavity. It is the the force balance between these different parts of the helmet structure and its interaction with the open-field exterior as well as with its everchanging lower atmosphere, which determine its equilibrium and stability. In Section 3, we take up the issues of how such a structure may eventually lose that equilibrium and stability.

### 3. Coronal Reconfiguration

Both in the large and small scales, the corona evolves significantly over an eleven-year cycle. The corona of 1980, shown at eclipse in Figure 2(a) is at the height of solar activity when the Sun has lost its magnetic dipole moment. It is strikingly complex compared to the near-minimum ‘dipolar’ corona of 1994 shown in Figure 2(b). The maximum-activity corona of 1991 observed by the *Yohkoh* soft X-ray instrument shortly after launch is shown in Figure 5 for comparison with the soft X-ray corona of 1994 near activity minimum (Ogawara *et al.*, 1992). This comparison shows the dramatic change of the corona on the (smaller) scales of the X-ray structures. The structures are more profuse and complex at activity maximum than at activity minimum. This change in the corona proceeds with fits of plasma activity of a broad range of time and length scales, ranging from the quiescent heating of the corona, through the complex highly nonequilibrium processes of the flare, to a rich variety of mass ejections. However, a point to emphasize is that the corona even at high activity is not in a constant state of explosion (Low, 1994a). After the rapid energy release in a flare, some magnetic structure always forms or reforms to persist for a length of time long compared to the rise times of MHD instabilities. For example, a helmet streamer can form and persist for days to weeks at a time prior to its disruption. *So the corona evolves via constant formation and disruption of relatively long-lived structures.* The distinction between activity maximum and activity minimum is principally in the frequency of formation-disruption events. The same physical processes seem to be operating in the individual events. For examples, flares are basically the same throughout the solar cycle, and helmet structures generally have the basic three-part structures.

The challenge of understanding the physics of solar activity is therefore as much in the understanding of what coronal structures are and why they may persist with stability in between eruptions, as in the understanding of their eruption and energy release. Moreover, the corona does not evolve chaotically without a goal. It systematically evolves over the eleven-year period of each cycle to completely reverse its global dipole magnetic field. This is clearly driven by the solar dynamo. Hence, any physical understanding of coronal activity needs to explicitly accord a role for the dynamo injection of magnetic flux. The corona is an excellent electrical conductor. It is also voluminous and optically transparent. This is the part of the solar atmosphere where we have the best chance of seeing the tell-tale signs of the presence and the fate of the injected magnetic flux. A case in point is the phenomenon of coronal mass ejections (CMEs) discovered in the seventies (Fisher, 1984; Hildner, 1992; Howard *et al.*, 1985, 1986; Hundhausen, 1988, 1995b; Kahler, 1992; Low, 1990, 1993b, 1994a, b; MacQueen, 1980).



September 15, 1991

September 15, 1995

**YOHKOH Soft X-Ray Telescope**

*Figure 5.* The solar corona observed on September 15, 1991 (a) and September 15, 1995 (b) using the soft X-ray instrument on the *Yohkoh* satellite (Ogawara *et al.*, 1992), showing, respectively, the profusion of bright structures near activity maximum (1991) and a conspicuous absence of bright structures near activity minimum (1995). This instrument observes thermal X-rays at temperatures in excess of about  $3 \times 10^6$  K. In (a), the bright features are either flares in progress or highly heated magnetic structures evolving relatively more slowly.

### 3.1. CORONAL MASS EJECTIONS

As often as twice a day, a large-scale structure in the corona disrupts and is ejected out of the corona at speeds ranging from 10 to  $10^3$  km s $^{-1}$  (Gosling *et al.*, 1976, 1994; Hundhausen, Burkepile, and St. Cyr, 1994). Each event carries a total mass in the range  $10^{15-16}$  g (Howard *et al.*, 1985; Hundhausen, 1995b; Hundhausen, Stanger, and Serbicki, 1994; Illing and Hundhausen, 1986). The contribution of coronal mass ejections to the solar mass loss is of the order of a few percent of the mass loss due to the more or less steady solar wind (MacQueen, 1980; Webb and Howard, 1994). Compared to other kinds of episodic mass ejections like the H $\alpha$  surges, flare sprays, spicules, etc., CMEs are distinct in two ways. Each CME is far more massive than any of these other mass ejections, and the mass in a CME almost always leaves the Sun. A CME liberates an energy of the order of  $10^{31-32}$  erg, in the form of the work done to lift its mass against gravity and to produce the kinetic energy of the expelled mass (Hundhausen, Stanger, and Serbicki, 1994; Illing and Hundhausen, 1986). This energy is comparable to that of a flare, putting the CME with the flare as the two most energetic phenomena in the corona. A point to be made significant later is that CMEs and flares liberate energies in two distinct forms (Low, 1994a). In the case of a flare, much of its energy manifests itself finally as thermalized or dissipated energy; the net result in this case is the intense heating

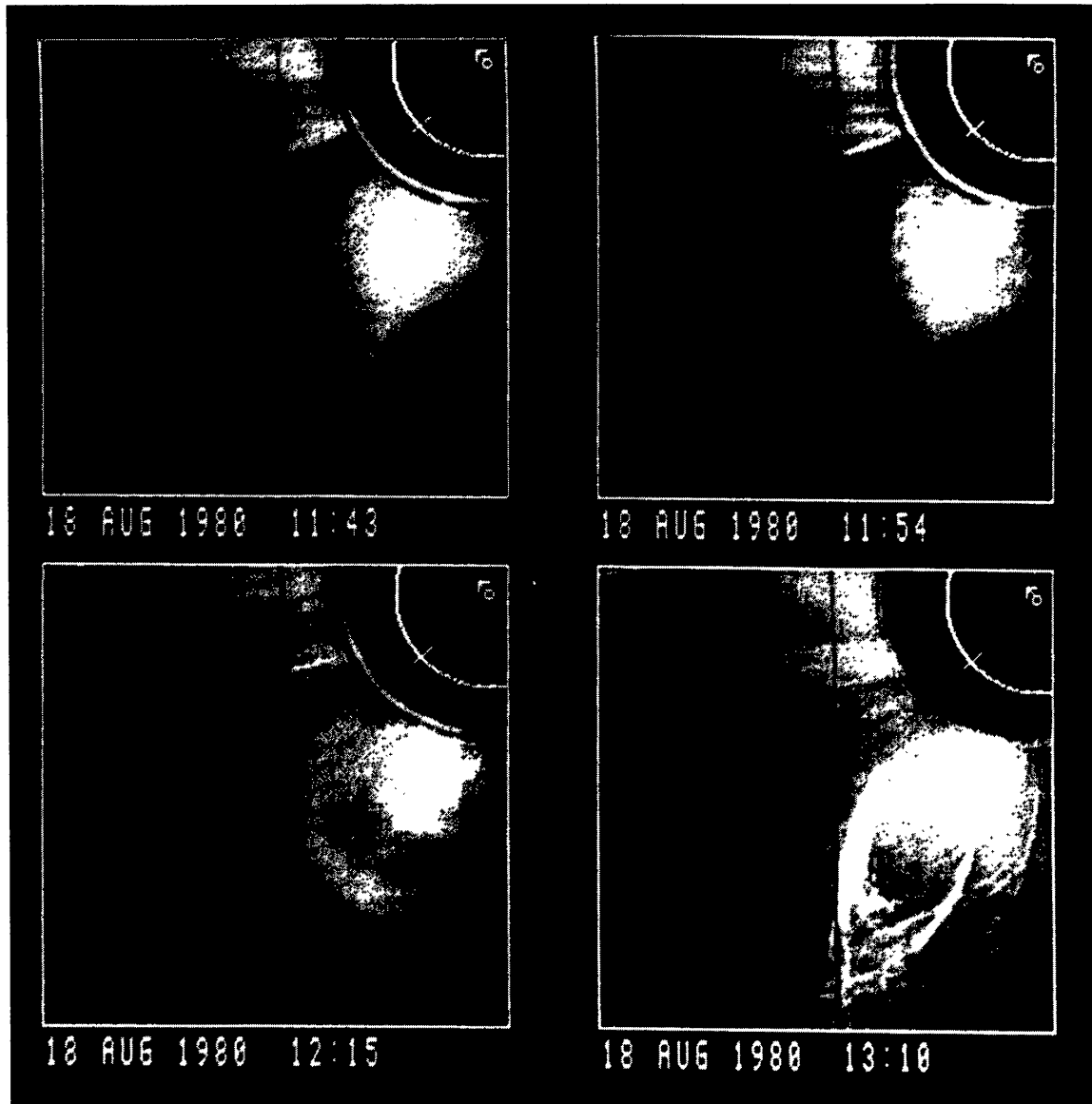


*Figure 6.* The August 18, 1980 CME observed in white light using the NASA Solar Maximum Mission coronagraph, with a field of view from  $1.6 R_{\odot}$  to  $6 R_{\odot}$  (Hundhausen, 1995b; Illing and Hundhausen, 1986). This CME displays the three-part structure of the leading shell, cavity and erupted prominence. The leading shell moved at a speed of about  $500 \text{ km s}^{-1}$ , which is moderately above average, carrying masses of the order of  $10^{16} \text{ g}$  in the shell and prominence, which make this CME one of the more massive observed by the SMM instrument.

of the corona. In the case of a CME, the energy liberated is in the ordered form of macroscopic work and bulk kinetic energy.

Many CMEs originate from the disruption of a helmet streamer (Hundhausen, 1995b; Illing and Hundhausen, 1986). Figure 6 shows an example observed in white-light using the coronagraph on the SMM satellite (Hundhausen, 1995b; Illing and Hundhausen, 1986). In the sequence of events shown, a pre-existing helmet streamer bursts forth to form a coherent structure travelling out at a speed of about  $500 \text{ km s}^{-1}$  at its leading edge. This CME shows the typical form of a bright leading shell of material surrounding a dark cavity within which an erupted prominence is found (Crito, Picat, and Cailloux, 1983; Hundhausen, 1988). The

three parts of the CME can be identified with the bright dome, cavity and quiescent prominence of the pre-eruption helmet streamer. (When a mass is quoted for a CME, it is customary to give the mass of the leading bright shell which is the disrupted dome of the pre-eruption helmet. In some cases, the erupted prominence trailing behind the leading bright loop may contain just as much or more mass but usually it has an order of magnitude less mass than the latter.) In the event in Figure 6, both the leading bright shell and the erupted prominence have masses of the order of  $10^{16}$  g, the latter with 50% more mass than the former (Hundhausen, 1995b; Illing and Hundhausen, 1986). This particular mass ejection is among the more massive observed during the SMM period.

In the low corona, the typical magnetic field strength is about 10 G based on simple extrapolations from measured photospheric fields or from interplanetary fields measured at earth orbit. Under typical coronal conditions, this field strength gives an Alfvén speed of  $700 \text{ km s}^{-1}$  or higher. The sound speed of a  $2 \times 10^6 \text{ K}$  plasma is about  $150 \text{ km s}^{-1}$ . While CMEs have speeds in the broad range mentioned above, the median speed is about  $350 \text{ km s}^{-1}$  (Gosling *et al.*, 1976; Hundhausen, Burkepile, and St.Cyr, 1994; Hundhausen, Holzer, and Low, 1987). Hence most CMEs move at supersonic but sub-Alfvénic speeds. These CMEs are not likely to produce fast MHD shocks in the corona, although their disturbance fronts may rapidly steepen into fast shocks further out in the corona (Sheeley *et al.*, 1985). On the other hand, slow and intermediate MHD shocks may form just ahead of CMEs in the low corona (Steinolfson and Hundhausen, 1989, 1990; Hu *et al.*, 1990). These varieties of shocks may be responsible for the characteristic inverse-concavity often observed at the CME front (Hundhausen, 1995b; Hundhausen, Holzer, and Low, 1987). Very fast CMEs moving at speeds of  $10^3 \text{ km s}^{-1}$  would produce fast MHD shocks in the low corona. Such CMEs are few in number (Sime and Hundhausen, 1987).

The gravitational escape speed at heliocentric distance  $\sim 1.1 R_\odot$  is about  $550 \text{ km s}^{-1}$ . It is remarkable that many CMEs move out at well below this escape speed, indicating that magnetic and pressure forces are continuously driving the CME as opposed to a ballistic expulsion (Low, 1984). There is a considerable amount of velocity dispersion, the leading part moving faster than the trailing part by as much as a factor of 2 (Illing, 1984; Low and Hundhausen, 1987). Although acceleration is not uncommon, the different parts of a mass ejection often move at constant speeds. The truly slow CMEs moving at steady speeds below  $100 \text{ km s}^{-1}$  provide clear evidence that they evolve from structures under stress that gradually get out of equilibrium, as opposed to being driven out of the corona by an impulsive input of energy (Forbes, 1992; Low, 1981, 1984; Mikić and Linker, 1994; Sime, 1989; Steinolfson, 1988, 1991; Wolfson, 1982; Wolfson, Conover, and Illing, 1987; Wu *et al.*, 1995). That such a dynamical evolution over a large range of speeds is possible has been demonstrated by a family of solutions describing a  $\gamma = \frac{4}{3}$  polytrope undergoing self-similar, time-dependent, MHD expansion in a  $r^{-2}$  gravity, with a velocity dispersion resembling that observed in CMEs (Illing, 1984; Low,

1984). These solutions in both 2 and 3 dimensions illustrate, by explicit examples, how the hydromagnetic equations allow the Lorentz, pressure, and gravitational forces to equilibrate everywhere in a CME during the motion so that each piece of the CME may move at a constant Lagrangian speed.

### 3.2. FLARE–CME RELATIONSHIP

Early in the study of CMEs it was found, and later studies confirmed it, that a great many CMEs occur in association with prominence eruptions and flares in their vicinities (Munro *et al.*, 1979; Sheeley *et al.*, 1983; Webb and Hundhausen, 1987). The association with eruptive prominences is not surprising since many of the CMEs originate from the disruption of a pre-existing helmet streamer with a prominence at its base. The association with flares raised a more interesting question.

A simple and attractive scenario was proposed in the late seventies that a CME is the part of the corona expelled out by the energy of the associated flare (e.g., Dryer 1982; Dryer and Wu, 1985). Early thinking on the solar origin of geomagnetic storms led to the suggestion that a flare might send off a blast wave into interplanetary space to disrupt the Earth's magnetosphere upon arrival (Hundhausen, 1972; Parker, 1963). When CMEs were discovered, it was natural to suggest that the CME might be the blast wave in the above scenario. However, observation does not support this suggested identification (Gosling, 1993a, b; Hundhausen, 1988, 1995b; Hundhausen *et al.*, 1984; Sime, MacQueen, and Hundhausen, 1984, 1985).

To begin with, those CMEs moving at extremely low speeds certainly do not fit the description of a blast wave. Careful analysis of the faster moving, typical CMEs show that they also do not have the properties of blast waves. In a few cases where it is possible to identify an MHD wavefront in the white-light observations, it is found that the wavefront is quite distinct from the CME (Sime and Hundhausen, 1987). This is quite consistent with the fact that the CME in most cases is a pre-existing structure which has broken away, as opposed to a dynamically and impulsively created wavefront. Moreover, CMEs with or without an associated flare do not look significantly different in white light, suggesting that CMEs and flares are distinct processes (Low, 1981).

Association of occurrences alone, of course, does not imply any particular causality between two events. To address the question of causality, Harrison (1986, 1991) examined CMEs and their associated flares observed by the SMM instruments. It was found that in all cases of clear association examined, the flare associated with a CME began some 20 minutes after the CME had erupted. This result has been confirmed by Hundhausen (1988, 1995b) using the combined observations of the SMM coronagraph and the Mauna Loa coronameter to bring the field of view down to  $1.2 R_{\odot}$  and thus reduce the uncertainty in the observed start times of CMEs. In all cases, the CME precedes the associated flare by minutes to an hour. Figure 7 shows an example where the heights of the different parts of a CME are

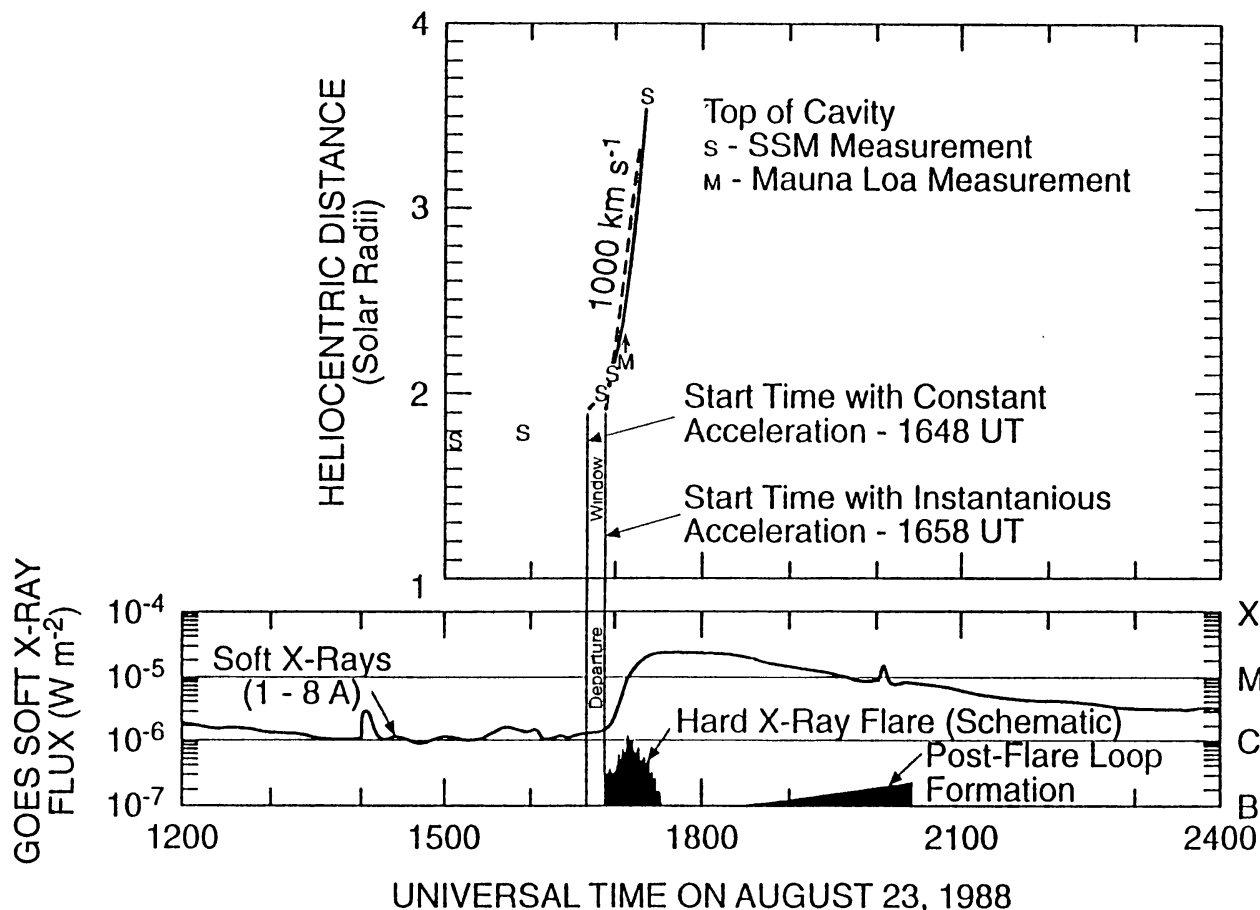
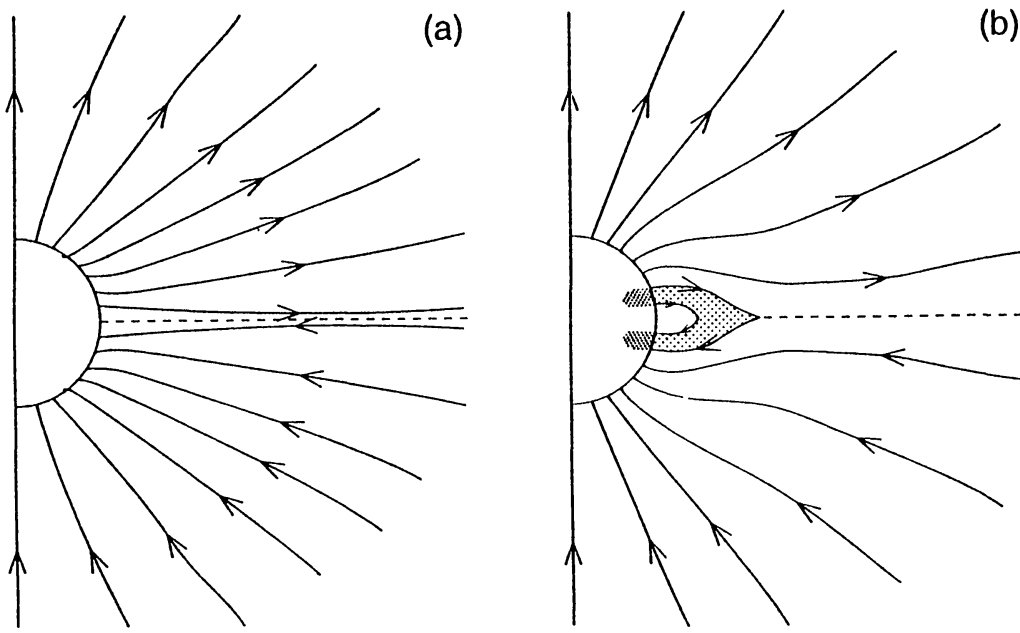


Figure 7. Study of CME-flare temporal relationship taken from Hundhausen (1995b). Heliocentric positions of the top of the cavity in the August 23, 1988 CME (*top panel*), as measured on a time sequence of 5 Solar Maximum Mission coronagraph images, with a single lower limit from the High Altitude Observatory – Mauna Loa coronameter image of the same CME. The NOAA GOES full-disk soft X-ray and several other flare emissions, as indicated, are shown in the bottom panel. This study shows that the cavity of the CME which trails behind the high density part of the CME is already moving at a speed abnormally high for a CME into the outer corona by the time the associated flare sets in as indicated by the rise of the soft X-ray flux.

shown on the same time line as the rise of the full-disk soft X-ray output of the Sun due to the associated flare (Hundhausen, 1995b). We can see in Figure 7 that the total energy of the flare actually took hours to be dumped into the atmosphere, long after this unusually fast CME has departed from the corona. Thus it is reasonable to conclude that the flare energy liberated did not play a role in the acceleration of the CME. This ordering of events is typical of many flare-associated CMEs on which comprehensive data are available.

The *Yohkoh* satellite allowed for the first time the imaging of a CME in soft X-ray at temperatures of about  $3 \times 10^6$  K and higher. No coronagraph has been available in space after the demise of the SMM satellite in 1989, but white-light observation of the corona from the ground at Mauna Loa continues. A number of CMEs have been observed simultaneously by the *Yohkoh* soft X-ray and the Mauna Loa white-



**Figure 8.** The magnetic-reconnection scenario as the origin of the two-ribbon flare. The fully open, axisymmetric, dipolar magnetic field (a) contains a current sheet in the reversal layer of the field at the equator. In the low corona where the plasma  $\beta$  is small, the sheet naturally collapses to result in magnetic reconnection. The closing of the open field by successive reconnection forms a growing region of closed bipolar magnetic fields (b). The newly reconnected bipolar fields are highly energized, which explains the soft X-ray bipolar loops (shaded part of the magnetic lines) of this type of flares. The chromosphere at the feet of these bipolar fields (the shaded region on the solar surface) responds with enhanced emissions, giving the signature feature of the two ribbons. As more newly reconnected loops form, others which formed earlier cool to form H $\alpha$  post-flare loops.

light instruments (Hiei, Sime, and Hundhausen, 1994). Meaningful comparison of the X-ray and white-light images can be made, provided it is recognized that the collision-dominated X-ray emissions of the corona drop in intensity more rapidly with heliocentric distance than the Thomson-scattered white light. The quiescent helmet streamer, especially one located in the high latitude away from the active region, appears as a faint structure in soft X-rays near the threshold of detection. When such a helmet streamer disrupts into a CME, some faint outgoing features may be identified in soft X-ray but nothing like the spectacular form of the CME in white light is observed. Only the post-CME flare shows up in soft X-rays as highly heated plasma in a newly formed helmet like mount minutes to hours after the white-light CME has left the corona. These simultaneous observations thus not only confirmed the results of Harrison and Hundhausen in a direct manner, but also raised an interesting theoretical point. They imply that the CME is largely an ideal or non-resistive MHD process, taking place at the high temperature of the quiescent corona, not involving sudden intensive dissipative heating of the coronal plasma. Intensive heating takes place only in the post-CME flare.

A point of clarification: there are more flares occurring in the corona than there are CMEs. The flares associated with CMEs are almost all of the type known as the two-ribbon flares (Tang, 1985; Švestka, 1976; Zirin, 1988). Long recognized, these flares can be interpreted in a well-known paradigm sketched in Figure 8 (Hirayama, 1974; Kopp and Pneuman, 1976). Beginning with a fully open bipolar magnetic field in the corona as shown in Figure 8(a), the magnetic field would readily reconnect to close itself to reach the state shown in Figure 8(b). Heating by this magnetic reconnection process may explain the following flare properties. The closing of open fields would produce new bundles of closed bipolar field to increase the size of the closed-field region. The newly produced fields forming at the boundary of the closed-field region will be hot and X-ray emitting while the older bipolar fields in the interior of the closed-field region would have cooled out of the X-ray regime and be emitting in a chromospheric line like H $\alpha$ , the latter being the classical H $\alpha$  post-flare loops.

This paradigm had a problematic aspect, unresolved until CMEs became known. The problem is that the stretching out of a coronal magnetic field into an open configuration like the one shown in Figure 8(a) requires work to be done on the magnetic field before that work can be released in a flare by the magnetic reconnection of the open field. An agent is needed for the role of opening up the initially closed magnetic field – observationally, the CME fits just this role (Hundhausen, 1988, 1995b; Low, 1981, 1982b, 1984, 1994a). The observed temporal ordering of the CME and its associated flares then makes physical sense. This leads us to the question of what triggers the CME. To deal with this question requires the consideration of the storage of magnetic energy in the corona.

### 3.3. CME MECHANISMS

Prior to its disruption as a CME, the streamer of a helmet structure is known to swell over a few days (Hundhausen, 1993; Poland and MacQueen, 1981). To observe how a helmet disrupts, however, we need to observe down at the base of the corona. Mauna Loa observations reveal several cases in which the CME eruption begins with the rise of the prominence cavity, with speeds at first below 100 km s $^{-1}$  and then accelerating to well above that speed, at which point, the dense dome of the helmet disrupts (Fisher and Poland, 1981; Fisher, Garcia, and Seagraves, 1981; Illing and Hundhausen, 1985, 1986). Helmet structures normally extend over several hydrostatic scale heights in the low corona. The cavity is naturally buoyant in the stratified atmosphere and is held in equilibrium both by the weight and bipolar field in the helmet dome, and by the weight of the prominence inside the cavity (Low and Hundhausen, 1995). When this equilibrium cannot be maintained or is destabilized, the cavity would naturally rise buoyantly (Low, 1981; Low, Munro, and Fisher, 1982; Wolfson, 1982; Wolfson, Conover, and Illing, 1987).

Prominences are not truly static, with constant dribbling of prominence material out of the system (Tandberg-Hanssen, 1974). The lost material is replenished by

various processes still not well understood, but such replenishment must take place to account for the observed relatively long life of the prominence. Fluctuations in the replenishment of prominence material may be an important driver of the prominence evolution. If the prominence weight increases, the effect is not dramatic for the prominence merely weighs further upon the cavity flux rope supporting it. A decrease of the prominence weight, even by small amounts at a time, has a more dramatic effect. As the prominence lightens, the large-scale magnetic topology is not changed and the cavity flux rope will gradually rise into the atmosphere to strain at the overlying magnetic structure as its anchor lightens. This may be the origin of the gradual rise of a crown filament in height as it first appears on the east limb, travels across the disk, and appears on the west limb, that is, if it survives for a half rotation. It is also known that such gradual ascension usually terminates in the filament's eruption, nowadays recognized to take place in association with a CME (Hundhausen, 1995a).

In this process, the role of magnetic flux rope of the cavity is dynamically crucial. The prominence may of course become unstable on its own in the process. In that case, the instability merely accelerates the loss of equilibrium to the cavity flux rope. As the flux rope rises and expands the helmet dome, the expansion has the immediate effect of weakening the confining magnetic field. The plasma of the helmet, upon losing confinement, expands out into interplanetary space. The CME therefore results from the breaking up and free expansion of the helmet plasma rather than by an impulsive release of energy. The CME speed is dependent on the nonlinear development of the large-scale flow of the CME, rather than being set at the fastest MHD speeds in the case of an impulsive input of energy. In the ensuing outflow, the flow may be driven by the expansion of the cavity flux rope as well as the thermal energy of the originally confined plasma. The prominence is dragged out by the embedding cavity. This relationship also explains qualitatively the observed dispersion of the speeds of the different parts of the CME with the trailing part moving more slowly than the leading part.

A theory for the combined CME-flare event must explain the origin of the large amount of energy involved. About as much energy is carried away by the CME as is left behind in the open magnetic field to be released subsequently during the post-CME flare. This total energy needs to be stored in the magnetic field prior to eruption, since the CME moves too fast to be directly driven by the photosphere moving at typical speeds of about  $0.5 \text{ km s}^{-1}$ . A theory of how this energy demand might be met in the corona has been developed successfully recently, but only after several theoretical issues about energy storage had been sorted out as described below.

The slow-moving photosphere can induce a field-aligned electric current into the corona. This way of building up energy in the corona was deemed promising in many publications (e.g., Barnes and Sturrock, 1972), but it has turned out that field-aligned currents alone are not adequate to store the energy required by the CME-flare process. It is instructive to see the physical reason for this inadequacy.

The energy problem posed by the field-aligned currents is treated in terms of whether a force-free magnetic field  $\mathbf{B}$  satisfying Equations (1) and (2) may have an energy in excess of the energy of an open state in which all lines of force are opened out to infinity with the footpoints of the field fixed at the photospheric boundary. If such a force-free field should exist, one may imagine it is produced by the photospheric displacement of magnetic footpoints, starting with some suitable initial state. Upon attaining this high-energy equilibrium, instability or nonequilibrium may initiate an outward motion driven by its stored energy to open up the magnetic field. Attempts to construct such a force-free field was abandoned when it was shown from general and particular considerations that the energy of the open field is always larger than any force-free field having the same boundary flux distribution at the photosphere (Aly, 1984, 1991; Sturrock, 1991). Therefore, when a magnetic field is progressively stressed to evolve through a sequence of force-free states, its energy may increase monotonically but is always bounded above by the energy of the fully open state. This means that the quasi-statically evolving field could, at best, approach the fully open state without ever having enough energy to spontaneously open up, let alone deliver the enormous amount of energy to drive a CME.

In general, the evolution does not even get close to the fully open state before a nonequilibrium sets in to convert it into a partially open (as opposed to a fully) open magnetic field (Low, 1986; Wolfson and Low, 1992). If the partially-open field is subject to further stressing, the field would generally encounter further opening of its closed portion of the total flux, but its total energy would still remain bounded by the energy of the fully open state (Low and Smith, 1993). An important qualification on this maximum energy result is that it applies only for force-free magnetic fields with all lines of force anchored to the base of the atmosphere. The relevance of this qualification will be apparent as our discussion proceeds.

The physical essence of Aly's constraint is that a magnetic field in an infinite domain without the presence of any other body forces, generally expands outward to seek new force-free equilibrium states when subject to progressive stressing (Klimchuk, 1990). This outward expansion puts a limit to the local build up magnetic energy density so that the total field energy cannot exceed the energy of the fully open state. If the magnetic field is confined within a finite region by rigid walls, progressive shearing of the field can lead to unlimited compression of the sheared field within the fixed space and, in this case, there is no limit to the energy the field may have. In the solar corona, gravity serves as a way of confining the magnetic field and preventing its unlimited expansion (Low, 1982b; Low and Smith, 1993). With a heavy enough atmosphere, a compressed magnetic field of any amount of energy may be built. In particular, such a magnetic field may acquire an energy exceeding that of the fully open state. This then is the key to building the necessary energy for a CME-flare. As we have pointed out, the plasma  $\beta$  is small only low in the corona. Over the scale lengths of the helmet streamer, both plasma pressure and weight are significant. The confining effects of the plasma, through its pressure

and weight, on the magnetic field involves not just field-aligned currents but also currents flowing across the magnetic field; the latter gives rise to the Lorentz force acting on the plasma.

There is another fundamental way of increasing the magnetic energy in the solar atmosphere, which is to introduce fully detached magnetic fields in the form of a flux rope. The fully detached magnetic fields can give up all of their energies by leaving the atmosphere and expanding to infinity. In contrast, magnetic fields anchored to the surface of the Sun eventually suffer stretching and take up energy in order to attain the highly stressed open state. Aly's constraint does not apply to a force-free field containing detached fields, in addition to the fields which are anchored at the solar surface. In that case, the energy associated with the detached field may plausibly permit the energy of the total field to exceed the energy of its fully open state. However, that excess has a definite severe upper bound because the anchored part of the force-free field can only confine a limited amount of detached flux (Low and Smith, 1993).

On the other hand, if gravity is present, its confining effect removes the upper bounds on both the amount of detached flux admissible and the associated additional energy. It follows naturally from our analysis that the helmet cavity, identified as a magnetic flux rope, is likely to be the crucial agent which enables the global magnetic field to store the high energy needed for the CME-flare. The energy residing in the cavity is kept at a high level by its confinement under the dense part of the overlying helmet. Closed-form axisymmetric solutions to Equation (3) have been obtained recently, involving pressure, gravitational, and Lorentz forces to model the coronal helmet with its cavity (Low and Smith, 1993). These solutions demonstrate that under the expected coronal physical conditions, the necessary amount of magnetic energy needed for the CME-flare can be stored. We have thus arrived at the necessity of the helmet cavity being a magnetic flux rope from yet another consideration different from the one relating to prominence structure.

The topological distinction between anchored bipolar magnetic fields and detached magnetic fields is absolute in axisymmetric geometry. In realistic situation, with no special symmetry, these two types of fields are the two extremes of a spectrum of field topologies exhibited by a magnetic flux rope anchored at two ends, with its lines of force winding a number of times about the rope axis in the corona. Despite the anchoring of the ends of these lines of force, one or several full turns of these lines of force about the rope axis behave like detached magnetic fields in being able to expand out to deliver its magnetic energy as work done on the plasma. Conceivably, the twisted part of the field may open up if its twist is extreme, while the rest of the field remains closed. This is a general form of the partial opening of magnetic fields treated by Low (1986) and Wolfson and Low (1992) under the assumption of axisymmetry.

It should be noted that the importance of pressure and gravity in the above storage of magnetic energy implies that the energies of these other forces must also be important for the CME. Although the magnetic contribution to the total

CME energy is expected to be dominant, plasma internal energy and possibly the ubiquitous heating of the corona must also make significant contributions which are not possible to estimate quantitatively at the present for want of observational information (Low, 1993b).

### 3.4. ORIGIN OF THE CAVITY FLUX ROPE

Accepting that the helmet cavity is a magnetic flux rope, what is its origin? One possibility is that it is produced in the corona from pre-existing bipolar magnetic fields, a process treated in various forms in the literature (Choe and Lee, 1992; Inhester, Birn, and Hesse, 1992; Martin, 1989; Pneuman, 1983; Ridgeway and Priest, 1993; van Ballegooijen and Martens, 1989). Generally, a converging and shearing photospheric motion together with magnetic reconnection may produce detached magnetic fields or a flux rope in the atmosphere. While such a process is theoretically viable, a number of observations and theoretical considerations suggest that this process does not create the cavity flux-rope in the corona. Instead the coronal flux rope may have a sub-photospheric origin (van Ballegooijen and Martens, 1990).

Consider the prominence magnetic field as a two-flux system, one being the flux linking the bipolar regions on the photosphere below and the other the axial flux of the prominence flux rope. If this flux-rope is produced in the corona by the traditional footpoint-displacement models, the sign of its axial field is determined from the initial bipolar lines of force by the sense of the photospheric displacements of the two footpoints. Consider the action of surface differential rotation on a bipolar field in the high latitude of the Sun. As Figure 9 shows, the axial field (the field component along the arcade) produced is of one sign in one case when the north polar field is positive and of the opposite sign when the north polar field is negative, say, a solar cycle later. In either case, the sense of twist of the helical lines of force are the same by the right-hand rule. So, as shown in Figure 9, the flux rope produced by magnetic reconnection in association with surface differential rotation has a positive helicity in the northern hemisphere independent of solar



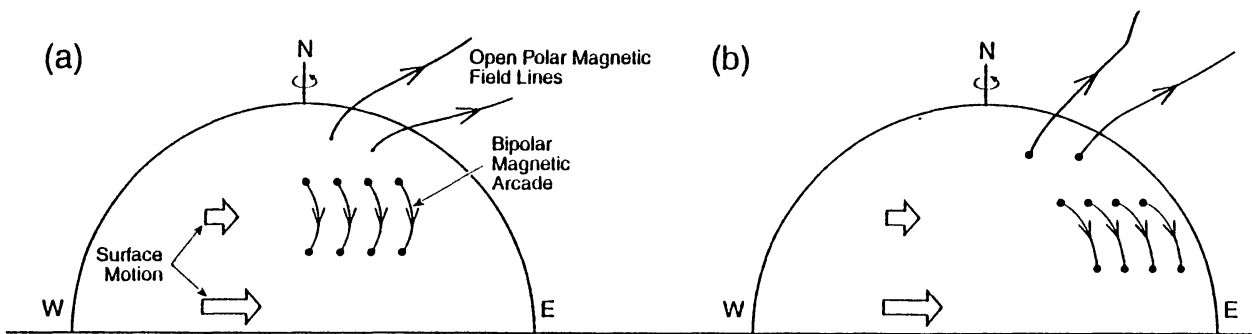


**Figure 9.** A schematic sketch of the relationship between the sign of the axial field in a sheared, bipolar magnetic arcade and the shear of the footpoint motion due to differential surface rotation in the northern solar hemisphere. The east–west oriented magnetic arcade, made up of 4 bipolar lines of force, indicated by the arrowed lines, is located at mid-latitude. Such an arcade usually contains a quiescent prominence, not shown in these sketches for simplicity. Starting from the initial unsheared state (a), the higher rate of surface rotation near the equator results in the set of footpoints nearer the equator moving ahead of the other set of footpoints. Under the frozen-in condition of high electrical conductivity, the magnetic field of the arcade acquires an axial field component along the arcade as shown in (b). Given the sense of the bipolar field in the initial configuration, the axial field component points east, so that the field has a right-handed twist down the arcade. If the global field is reversed in direction, the shearing process would still produce a right-handed twist down the arcade. As noted by van Ballegooijen and Martens (1990), this sense of the twist in the northern hemisphere does not agree with observations in general.

#### 4. The Nature of Solar Activity

The photosphere and chromosphere are much more complex to interpret than the large-scale corona. In these dense lower parts of the atmosphere, complicated radiative-transfer processes stand in the way of a simple interpretation (Athay, 1988; Zirin, 1988). This complication is compounded by the fact that at the photosphere, the magnetic field is in the form of discrete flux tubes of diameters smaller than the limit of optical observational resolution of about 1 arc sec (Parker, 1979; Stenflo, 1994; Steiner, Knoelker and Schüssler, 1994).

In this section we will not deal with all aspects of photospheric and chromospheric observations, except those relevant to the physical picture described in the previous two sections. We will construct a relationship between the corona and the lower levels which can relate hitherto disjoint sets of observations.

When a magnetic field emerges from the interior into the atmosphere, the plasma it contains cannot immediately mix with the background atmosphere because of high electrical conductivity. Consequently electric current sheets form and dissipate resistively in a state of fully developed turbulence that persists until a metastable state of equilibrium is established (Canfield, Priest, and Rust, 1974; Low and Wolfson, 1988; Martin, 1980; Rust, 1976; Zirin, 1988). This clearly is the physical nature of flares associated with the emergence of new magnetic flux, although its physics is extremely complicated (e.g., de la Beaujardière *et al.*, 1995; Forbes and Malherbe, 1986; Livi *et al.*, 1989; Masuda *et al.*, 1994; Moore *et al.*, 1984; Tanaka, 1991; Tsuneta, 1996a; Tsuneta *et al.*, 1992; Wang, 1994; Zirin, 1983).

In the chromosphere, say, as observed in the H $\alpha$  line, the emerging flux appears as bipolar arches with materials draining down the two sides (Zirin, 1988). As the emergence proceeds, the magnetic structures generally take on a sheared or twisted appearance (Kurokawa, 1987; Leka *et al.*, 1996; Wang, 1992, 1994; Wang and Tang, 1993; Wang *et al.*, 1994). After the flaring activity has subsided, a dark filament usually forms over the polarity inversion line of the emerged field (Athay *et al.*, 1985a, b; Zirin, 1988). This filament is associated with a magnetic flux rope, as interpreted in the previous section, which must have either emerged through the photosphere or reformed after the turbulent flaring has subsided. The conclusion may therefore be drawn that a new magnetic field tends to emerge twisted and to settle, following the flaring activity, into a stable state which retains its twist (Hagyard and Rabin, 1986).

This behavior may be related to the approximate conservation of the total magnetic helicity in MHD turbulence. This conservation law is a powerful tool when applied to laboratory plasmas but may not be simply carried over for application to solar plasmas (Taylor, 1974, 1986; Low, 1985, 1994a). In recent years, there has been considerable interest in its application to solar and space physics (e.g., Aly, 1992; Berger, 1985; Heyvaerts and Priest, 1984; Kusano, Suzuki, and Nishikawa, 1995; Low, 1993c, 1994a, b; Norman and Heyvaerts, 1983; Rust, 1994; Rust and Kumar, 1994; Vekstein, Priest, and Steele, 1991). We therefore digress here to discuss the basic physics of magnetic helicity, before considering its applications to solar physics.

#### 4.1. MAGNETIC HELICITY AND MAGNETIC RECONNECTION

With perfect conductivity, the magnetic field is frozen-into the plasma. It follows from this property that the interweaving topology of the lines of force cannot change as the plasma evolves. Imposing a fixed interweaving topology of the lines of force is therefore another (equivalent) way of expressing the condition of perfect conductivity. This is accomplished by the use of the quantity called the magnetic helicity density:

$$h = \mathbf{A} \cdot \mathbf{B} , \quad (4)$$

where  $\mathbf{A}$  is the vector potential of  $\mathbf{B}$  (Moffatt, 1978). It is not a physical quantity because of its dependence on the free gauge of  $\mathbf{A}$ . So caution needs to be exercised in its use. In this subsection, we will describe its proper use, review its powerful application to the confined laboratory plasma, and, finally, show how it may or may not be used in application to the solar atmosphere.

Consider the total magnetic helicity in a volume  $V$ ,

$$H(V) = \int_V h \, dV . \quad (5)$$

This quantity still depends on the free gauge of  $\mathbf{A}$  except for those volumes of space bounded by magnetic flux surfaces. If  $V_M$  denotes such a magnetic volume bounded by a magnetic flux surface  $\partial V_M$ , then

$$\mathbf{B} \cdot \mathbf{n}|_{\partial V_M} = 0, \quad (6)$$

where  $\mathbf{n}$  is the surface normal vector. By a simple application of Gauss's theorem and the use of boundary condition (6), it can be shown that  $H(V_M)$  is independent of the free gauge. This physically meaningful quantity is a topological measure of the twist and inter-linking of the magnetic lines of force wholly contained within  $V_M$  (Moffatt, 1978). The measure is only meaningful for magnetic volumes because it requires the accounting of all linkages along the entire length of each line of force. Linkages among a set of lines of force are associated with the component of the electric current density along the magnetic field. The preservation of these linkages under perfect conductivity implies that a certain measure of the field-aligned current density cannot be removed. This does not mean that the field-aligned currents are conserved but rather that they will always change in time and flow in such magnitudes as to preserve the linkages. Note that the field-aligned currents do not generate the Lorentz force; this force arises strictly from the current component perpendicular to the field; see Equation (3). In contrast, the frozen-in condition does not require the volumetric cross-field currents to be preserved in any particular form. It is always possible to physically adjust the magnetic lines of force with no change in field topology such that the field is force-free (Equation (3)) everywhere except at surfaces of tangential discontinuities (Parker, 1994a).

In some laboratory devices, the entire magnetic field of the plasma is confined within a rigid container volume  $V$  so that its total helicity  $H(V)$  is a physically meaningful quantity. The application of magnetic helicity is simplest in such a plasma. Nested within  $V$  may be one, more, or an infinite number of magnetic volumes each of which is a topological invariant under the condition of perfect conductivity. As an aside, it is possible that  $V$  is the only magnetic volume in the case of a chaotic magnetic field in the form of a single line of force filling up  $V$  ergodically (Dombre *et al.*, 1986; Parker, 1979). In any case, as the plasma evolves, a magnetic volume,  $V_M$ , is well defined by a set of boundary magnetic flux surfaces which confine the same plasma particles for all time. It is in this sense that the invariant total helicity  $H(V_M)$  residing in  $V_M$  is carried along unchanged within the same parcel of plasma.

In the presence of resistivity, the magnetic lines of force may reconnect and the plasma may slip across magnetic flux surfaces. Reconnection changes the topological connectivities of magnetic volumes, splitting a volume into many or merging two or more volumes into one. Resistive slippage results in the local loss of helicity. In either cases,  $V_M$  and  $H(V_M)$  are no longer topological invariants. In a plasma of finite but very high conductivity, as characterized by an extremely large magnetic Reynolds number, resistive effects are only important at spatially localized regions where current sheets form and reconnection of magnetic lines of

force occurs. The resistive slippage of plasma across its magnetic flux surfaces is negligible in the plasma volume as a whole, so that helicity suffers little *in situ* loss but is redistributed principally via changing magnetic volumes as reconnection proceeds. Therefore, in the case of a plasma in a rigid container  $V$ , the total helicity  $H(V)$  in the container may be approximately conserved even if it is no longer meaningful to use  $H(V_M)$  because there is no invariant  $V_M$  within  $V$ . This conclusion can also be demonstrated for a highly conducting plasma by an inequality which sets the rate of decay of magnetic helicity to be significantly lower than the rate of magnetic energy dissipation, so that to a first approximation, the total helicity may be taken to be conserved (Berger, 1984).

The approximate conservation of  $H(V)$  was postulated by Taylor (1974) to explain the relaxed state of the reversed-field pinch observed at the end of a turbulent initiation. The plasma in this case is dominated by the magnetic field, the low  $\beta$  limit. Neglecting the plasma energy in this limit, the relaxed end-state must be one with a minimum in magnetic energy which conserves  $H(V)$ . Variational calculus identifies this end-state to be a force-free magnetic field satisfying Equations (1) and (2) with a proportionality constant  $\alpha = \alpha_0$  set to a value such that the field has the right amount of conserved magnetic helicity, subject to boundary condition (6) with  $V_M = V$  (Woltjer, 1958). Predictions based on this simple model are in excellent agreement with experimental data (Taylor, 1974, 1986).

The extension of Taylor's idea to the solar atmosphere with an infinite domain is not straightforward because of two principal obstacles (Low, 1985, 1994a). The first is that the magnetic fields in the solar atmosphere are not confined wholly within the atmosphere but are anchored to the solar surface so that we lose the gauge invariance of the total helicity in the atmosphere. This may be remedied formally by the replacement of the helicity with some suitable form of 'relative' helicity, explicitly made gauge-invariant (Berger and Field, 1986; Finn, 1986; Jansen and Chu, 1984). For the solar atmosphere identified with volume  $V$ , we have the boundary condition

$$\mathbf{B} \cdot \mathbf{n}|_{\partial V} = F(\partial V), \quad (7)$$

for a fixed surface flux distribution  $F$ . This surface flux distribution defines a unique potential field  $\mathbf{B}_{\text{pot}}$  in  $V$ . In one proposal, the twist in the magnetic field in  $V$  may be measured by the difference between the helicities of  $\mathbf{B}$  and  $\mathbf{B}_{\text{pot}}$  evaluated in some suitably chosen common gauge (Berger and Field, 1986). Once the common gauge is picked, the relative helicity is unchanged if the same gauge change is applied simultaneously to the vector potentials of  $\mathbf{B}$  and  $\mathbf{B}_{\text{pot}}$ . The requirement of a simultaneous change of gauge to both vector potentials appears artificial although the construction is a promising means of measuring the topological complexity of the lines of force of  $\mathbf{B}$ . The relative helicity so formulated is a measure of the topological departure of a field from its associated potential field. The two fields differ in terms of the linking of pairs of footpoints on  $\partial V$  by the lines of force and the interweaving of these lines inside  $V$ , if the relative helicity is not zero.

The other, more severe, obstacle comes from the infinite extent of the atmosphere. Suppose we accept the idea of relative helicity and ask for the corresponding Taylor state for a low- $\beta$  magnetic field outside a unit sphere on which a flux distribution is given as described by Equation (7). Variational calculus would again lead us to the force-free field with  $\alpha = \alpha_0$ , a constant, set to a value to produce the given relative helicity. There is ambiguity here because the relative helicity is dependent on the gauge used in the construction of the helicities of  $\mathbf{B}$  and  $\mathbf{B}_{\text{pot}}$ . But there is a separate and more basic concern. The appropriate boundary conditions on the force-free magnetic field are Equation (7) and the physically reasonable requirement that  $\mathbf{B}$  vanishes at infinity. Using the properties of the Helmholtz equation, it can be shown that, in general, the solutions for  $\alpha_0 \neq 0$  describe a magnetic field which has an infinite energy even if  $\mathbf{B}$  vanishes at infinity. The only exception is the potential field corresponding to the case of  $\alpha_0 = 0$ . This result has been known (Seehafer, 1978; Berger, 1985; Laurence and Avellaneda, 1993) but was given a physical explanation recently (Low, 1994a).

If we interpret the Taylor end-state to be one in which the twist in a magnetic field has been spread throughout the plasma interior by magnetic reconnection to seek a lowest-energy state, then it follows that the potential solution with  $\alpha_0 = 0$  is the unique Taylor state for the magnetic field in the infinite atmosphere, *irrespective of the total amount of twist in the atmosphere prior to relaxation*. This is simply the consequence of spreading any finite measure over an infinite domain. In such a spread of the magnetic twist, the local magnetic twist everywhere tends to zero and the relaxing field becomes indistinguishable from the potential field. During the turbulent relaxation under the condition of large magnetic Reynolds numbers, the plasma is non-resistive outside the reconnection regions, and communication between the different parts to bring about the relaxation can proceed only at the characteristic (finite) ideal wave speeds. For an infinite domain, the relaxation would therefore take a very long time; in principle, the relaxation time is infinite. In contrast, one may assume for most finite laboratory devices that communication between the different parts of the plasma takes place rapidly at these wave speeds.

We conclude that if Taylor's postulate is applied to the infinite atmosphere, the end-state of relaxation is the potential field, and, it would take an extremely long time for that end-state to be attained. If a magnetic flux were to emerge into the corona and the coronal base is then taken rigid to let the entire atmosphere have all the time to relax, this conclusion would be relevant. But this conclusion is not relevant because the real corona is far more complex, of course. Magnetic fields emerge continually, and, after emergence, they interact with each other and are continually driven by the ever changing lower atmosphere. Moreover, the low- $\beta$  approximation does not apply everywhere in the corona. The presence of gravity and pressure gradients make for far richer classes of metastable equilibrium states than those described by the force-free magnetic fields. All these considerations suggest that the rich variety of relatively long-lived magnetic structures observed in the solar atmosphere are metastable states following a flaring phase during

which excess energy is shed via magnetic reconnection. If this is the case, Taylor's postulate needs to be generalized beyond the low- $\beta$  approximation to explain the observed metastable states.

When a magnetic field emerges into the corona as a significantly twisted field, it flares to shed energy in order to rapidly seek a metastable state. Flaring changes the field topology, of course, but cannot remove a certain measure of the global magnetic twist, in consequence of the high electrical conductivity. While no theory is available at the present to state what that measure of conserved twist is and how it remains localized in the atmosphere, we may expect that the metastable state is characterized by a significantly twisted magnetic field. The commonly observed formation of a dark filament over the polarity inversion line following the emergence of a bipolar field fits this expectation. In the subsequent history of an emerged structure, more flarings may take place as the result of its interactions with other magnetic systems. The resultant metastable state forming out of the interacting systems would, by the same expectation, conserve the same measure of magnetic twist for the combined system. We will use this extension of Taylor's postulate to gain insight into solar phenomena in the rest of our discussion. We will refer to this extension simply as the conservation of magnetic helicity and not repeat the caution that a complete theory to make this conservation law specific is lacking at the present.

#### 4.2. THE HYDROMAGNETIC NATURE OF FLARES

The intensities of heating in the corona form a continuous and extremely broad spectrum, ranging from the nanoflares of small-scale reconnections to heat the quiescent corona, to the less frequent major X-ray flares. The observed spectrum of intensities appears to fit a power law suggestive of an avalanche process (Hudson, 1991; Lu and Hamilton, 1991; Lu *et al.*, 1993). In a general sense, flares are the reconnection processes by which a magnetic field in the solar atmosphere rapidly discharges its free energy to reach the nearest quiescent state.

The underlying physical mechanism is a fundamental property of highly conducting plasmas pointed out by Parker (1994a). Such a plasma is partitioned by the flux surfaces of its frozen-in magnetic field into volumes which cannot readily mix one into another if the magnetic field dominates, as is the case in the corona. These magnetic volumes tend to expand outward and press into each other to form magnetic tangential discontinuities, which dissipate resistively by reconnection to reduce the stress build up. In a lot of circumstances, this process proceeds continually on the small scales with only gradual large-scale changes. This has been proposed by Parker (1979, 1988, 1989, 1994a) to be the origin of quiescent heating in the closed-field regions of the corona. Other mechanisms of quiescent heating by waves also require the creation of extreme gradients in the magnetic fields in order to achieve a significant resistive dissipation rate despite the high conductivity of the hot corona (Zirker, 1993). The orders-of-magnitude larger amounts of

energy released in major flares are probably of the same basic mechanism (Low and Wolfson, 1989; Low, 1989), operating in a different manner. Conceivably, if the magnetic field is in a highly stressed metastable state with a great deal of volumetric currents, a loss of equilibrium could result in the creation of a magnetic tangential discontinuity which is neither weak nor spatially confined as expected in the case of quiescent heating. Then, in a typical Alfvén transit time (of the order of a few minutes in the magnetically dominated active-region corona), a significant fraction of the energy previously stored as a resistively stable volumetric current is converted into the discrete current in a magnetic tangential discontinuity. The latter then dissipates resistively, setting up a turbulence which produces more tangential discontinuities and further resistive dissipation. The basic process has the following two consequences of high electrical conductivity. It is the high conductivity which, in the first place, allows for stable magnetic-energy storage in the form of free flowing current densities built up over time without significant resistive dissipation. It is also the high conductivity whose constraint on the dynamics of the adjusting magnetic structures which brings about the extreme current densities in magnetic tangential discontinuities so that resistive dissipation sets in in spite of the high conductivity.

The above broad-brush picture of the different levels of heating in the corona is physically reasonable if all the flares and heating over a solar cycle are viewed collectively. The hard problems of flare physics lie in the quantitative understanding of the turbulent state of the flare in progress. The central tasks are the identification of the specific physical processes, both observationally and theoretically (e.g., Forbes and Malherbe, 1986; Masuda *et al.*, 1994). These are highly time-dependent processes complicated by the break down of the ideal-fluid description and by the fully nonlinear coupling between the fluid and particle behaviors. These complex problems lie outside the scope of this review. For our purpose here, the above broad-brush picture suffices for us to recognize that there are four stages in the history of a magnetic structure from the time it has emerged into the corona to its final demise. These stages are marked by flaring so that we might put flares into four distinct classes based on their physical nature or roles in the evolution of a magnetic field (Low, 1994b). This classification is different from the usual ones based on the observed characteristics of flares (Švestka, 1976; Zirin, 1988). The two are of course complementary.

The first class of flares is the low-intensity reconnection events on the small scales leading to quiescent heating, the nano-flares (Lu and Hamilton, 1991; Parker, 1988, 1994a). They do not result in reconfigurations of magnetic structures on the large scales, say, of the order of  $10^4$  km or larger, although the magnetic changes in the small scales may be expected to accumulate over a longer time scale to contribute to the evolution of the magnetic field.

The second class of flares results from the adjustments of magnetic fields upon emergence into the solar atmosphere. Flux emergence is the key feature of this type of flare (Martin, 1980; Rust, 1976; Zirin, 1983). The field usually emerges as

a twisted structure. The field which interacts with it is generally also twisted. The end state of such a flare generally retains the net twist of the total field, leading to the formation of a flux rope with a prominence embedded in it. So the formation of a prominence is a key feature of this type of flare.

The third class of flares occurs typically many times during the life time of a magnetic field already in the solar atmosphere. It may be due to a build-up of internal stress in the field by the photospheric motion of magnetic footpoints (e.g., Low, 1982a; Mikić and Linker, 1994), or due to the interaction of two or more magnetic fields brought together by large-scale photospheric motions (e.g., Chou and Low, 1994; Démoulin, Hénoux, and Mandrini, 1992; Tsuneta, 1996b). To the extent that these structures have a significant net magnetic helicity, a prominence may also form at the end of the flare. This class of flares coalesces many magnetic structures into one. The end product is a larger scale magnetic structure, much simplified in structure by repeated and successive flaring. We may think of these flares to be the ones that bring an active region to its decayed stage, characterized by its more extended photospheric area, weaker photospheric field strengths, and relatively straight and long polarity inversion lines (Gaizauskas *et al.*, 1983). These inversion lines have long quiescent prominences which locate high in the atmosphere.

Yet flaring does not end in this decaying phase (Dodson and Hedeman, 1970; Martin, 1980; Zirin, 1988). Indeed, some of the biggest flares occur in this phase, usually in the form of the two ribbon flares with eruptions of the long quiescent prominences. Nowadays we know that these flares are associated with CMEs (Hundhausen, 1995a, b), and, as a group, they form the fourth class. What distinguishes this class is that these flares are due to the reclosing of a magnetic field opened by the massive expulsion of coronal material into interplanetary space. In terms of magnetic helicity or twist, this class is distinctive in another way. Whereas, magnetic twists remain trapped in the fields undergoing the other types of flares, the opening up of the magnetic field in this fourth class allows the magnetic twist to propagate out as a non-resistive process along the opened field into interplanetary space. This means that the magnetic field by that process loses its magnetic twists (but see Gosling, 1993a) and the field, by reclosing, is allowed to settle into a more potential-like state with little or less magnetic twist. In this sense, this flare is a final throe of a decaying (combined) magnetic structure which finally has gotten rid of its magnetic twists accumulated from all the coalesced twisted structures which had emerged early in the history of an active region.

#### 4.3. THE HYDROMAGNETICS OF MAGNETIC-FUX EMERGENCE

Compared to the magnetic field in the photosphere and above, we are, of course, even less certain in our knowledge of the magnetic field in the solar convection zone. Helioseismology holds a glimmer of promise of some direct observational inference in the near future on magnetic structures beneath the photosphere, notably on the depth of penetration of the active region magnetic-field system (Bogdan and

Duvall, 1996; Duvall *et al.*, 1996). Until observation is able to provide useful information to constrain our ideas, theoretical consideration is only a guide (e.g., Choudhuri and Gilman, 1987; Ferriz-Mas and Schüssler, 1993; Fan, Fisher, and DeLuca, 1993; Moreno-Insertis, 1992; Parker, 1979, 1994b, 1995a–c; Schüssler, 1979).

Current thoughts are that the dynamo action takes place at the base of the convection zone, with layers of magnetic flux peeling off to buoyantly rise to the photosphere (Gilman, 1986; Parker, 1979, 1987). An idea very relevant to our concern in this paper is that the magnetic flux rising to the photosphere may be in the form of a largely closed magnetic system, probably enmeshed in a larger system (Lites *et al.*, 1995; Parker, 1994b; Spruit, Title, and van Ballegooijen, 1987). Such a structure may be either created as such by the dynamo in some suitable manner, or by reconnection and disengagement from the general toroidal field in the interior of the Sun. A disengaged, coherent field would explain the phenomenon of the delta sunspot. This is a sunspot with two umbrae of opposite magnetic polarities embedded in a common penumbra. It is known that a delta sunspot, once formed, often decays without separation of the two umbrae of opposite polarities (e.g., Zirin, 1988; Shi and Wang, 1994), suggestive of a closed magnetic system rising through the photosphere. A recent study of the measured vector magnetic fields at the photosphere of such a process suggests that a significant part of the closed magnetic system may rise clear of the photosphere into the corona (Lites *et al.*, 1995). Let us examine some theoretical implications of this process. This process is probably common in the solar atmosphere but is not well recognized because of the current popular notion that the coronal magnetic fields are principally bipolar arches with feet anchored in the dense photosphere. This notion is due in part to the now familiar photographs of the soft X-ray corona with its profusion of bipolar structures.

The high density and temperature of bright X-ray loops depend crucially on the connection of these loops to the photosphere which is the ultimate source of both energy and mass. A magnetic field which is disconnected from the photosphere or is connected by a tortuous magnetic path to the photosphere is denied ready access to the photospheric mass source, given that material cannot cross the magnetic field under the frozen-in condition. These types of magnetic geometry are found in a flux rope, and they promote thermal instabilities in its interior, evacuating the magnetic field to form a prominence trapped in the rope. So magnetic structures of the flux-rope type are neither dense nor greatly heated. Therefore, in X-rays, they are expected to appear as dark regions. Indeed, the soft X-ray corona shows two types of dark region, the coronal holes where the field is open to interplanetary space (Zirker, 1977) and the typically long lanes identified to coincide with the ( $H\alpha$ ) filament channels, on the disk, and with the cavity under the helmet streamer, at the limb (Serio *et al.*, 1978; McIntosh, 1972). Often a prominence is found in a filament channel. Hence, the prominences, filament channels, helmet cavity, and X-ray dark lanes are the signatures of a magnetic flux rope in the low corona.

If we accept that a magnetic flux rope is able to make its way through the photosphere, what are the dynamical signatures of this process? In particular, if a magnetic field is closed, how does it rid itself of the plasma it contains in order to break free to rise all the way into the corona? Magnetic buoyancy is the driver of this process as it is also responsible for the peeling of magnetic flux off the base of the convection zone to rise to the photosphere (Parker, 1955, 1977, 1979). The same buoyancy effect operates differently in the convection zone and in the solar atmosphere from the photosphere up. In the convection zone, the scales of the magnetic field is likely to be comparable to the scales of the fluid. The magnetic field is not expected to be so strong as to completely dominate the massive fluid it is embedded in. In fact, magnetic buoyancy itself is the mechanism which sets a limit ( $\sim 10^5$  G) to the strength which the field can have in the convection zone; fields are buoyantly expelled before they get stronger than the limit (Parker, 1977). In the solar atmosphere, magnetic buoyancy operates in a multi-scale medium. For a magnetic field extending from the photosphere into the corona, it has scales greatly exceeding the small ( $10^2$  km) photospheric hydrostatic scale height but comparable to the coronal hydrostatic scale height ( $10^5$  km). It also extends from a fluid-dominated, convecting photosphere to the tenuous, field-dominated, stably-stratified low corona. The effect of magnetic buoyancy in this complex atmosphere has not been fully explored theoretically although considerable modeling work has been pursued recently (e.g., Matsumoto *et al.*, 1993; Matthews, Hughes, and Proctor, 1995; Shibata *et al.*, 1990). In previous theoretical works, there has been a well-motivated tendency to keep the models simple by separating the coronal and photospheric aspects of the problem. One takes the photosphere to be an infinitely thin and heavy layer for coronal problems, or else, one deals with the photosphere and below without incorporating the corona into the model. To address the two questions posed at the beginning of this paragraph, we need to deal with the explicit coupling between the photosphere and the atmosphere above. Numerical simulation holds the only promise of treating this coupling quantitatively but the numerical resources required for modeling an atmosphere extending from the high to low- $\beta$  regions remains quite formidable. In the following, we point out some of the important qualitative effects that can cause a closed magnetic field to continue to rise into the corona after it has made its way through the convection zone.

Consider a closed magnetic field extending into the corona but threading through a certain depth below the photosphere. We may think of this field in the simplest case to be an ‘O’ loop, but such a field has to be very rare because most three-dimensional magnetic fields in the real world can have a strong chaotic component, with isolated closed field lines tangled with ergodic field lines (Dombre *et al.*, 1986; Parker, 1979). A ball of toroidal twisted field is an example of the latter (Lites *et al.*, 1995). In all these cases, the magnetic field is buoyant in the corona but is anchored by the dense photospheric and sub-photospheric plasma trapped at the base of the closed magnetic structure. Such a structure is generally unstable because the magnetic field behaves like a pressurized (through the magnetic pressure) gas with

no mass, and, therefore, always buoyant. In the photospheric region of the closed magnetic field, the horizontally oriented field is constantly agitated by turbulent convection and is susceptible to a form of the Parker instability (Parker, 1966; Mouschovias, 1974). As the instability develops, heavy fluid tends to flow along the local field to seek a lower gravitational potential. This draining of plasma depresses the magnetic valleys of the complicated field while the evacuated parts of the field become increasingly buoyant. As the instability runs away nonlinearly, the dense and heavy magnetic valleys may sink and break away by magnetic reconnection due to the formation of magnetic neutral sheets as proposed in Parker (1975). This process takes place as fast as reconnection permits, up to the Alfvén speed of the order of  $1 \text{ km s}^{-1}$  in the photosphere, which is a relatively slow process. In this manner, the closed magnetic field gradually loses its anchor in the photosphere, and, by its buoyancy, will pass into the corona.

It has been discussed in the literature that a magnetic field might be submerged back below the photosphere after its emergence (e.g., Parker, 1984; D'Silva, 1995). In the scenario we described above, there is also flux submergence. It is submergence not of an entire magnetic structure but of a *bottom* part of the structure which has collected, through drainage along the field, a significant portion of the plasma initially trapped in the structure. This heavy accumulation of plasma sinks and breaks away with its own trapped magnetic flux by reconnection, in order that the greater part of the original structure could rise buoyantly upward. The net effect is that of separating the magnetic structure from its otherwise frozen-in plasma. This process must be prevalent everywhere from within the convection zone out into the corona. There are special circumstances one might ingeniously conceive for an *entire* magnetic field to be submerged deep into a stratified fluid, but they have to be freak events in the chaotic natural environment; whereas, the above process systematically and progressively causes a magnetic structure to lose its entrapped mass from the magnetic bottom and rise buoyantly. The point to realize is that the part of a magnetic field which has entered the corona finds itself in a very tenuous, practically perfectly conducting medium. No amount of ‘pulling’ at the photosphere and below can physically get this large-scale coronal field back down.

There is a second effect which helps to lighten the buoyant magnetic field. Not every magnetic valley in a complicated magnetic field necessarily gains weight in a fully developed Parker instability. The siphon flows along the magnetic lines of force is produced by the tendency to equilibrate the hydrodynamic forces along the field. This in general tends to drain all material into the gravitationally *deepest* magnetic valley at the expense of the other magnetic valleys in a locality. For a flux rope of helical fields, for example, the siphon draining along the helical field lines tends to collect mass at a local sag in the flux rope while the rest of the helical field, with its helical crests and valleys, rises up in the atmosphere.

The siphon effect can collect plasmas in a length of magnetic flux undulating in the photosphere (and below) and dump it in a few select magnetic valleys. It can

also siphon mass up a field which extends into the chromosphere and corona, say, in the case of a helical field extending well above the photosphere, to dump the mass elsewhere back in the photosphere. The latter effect is probably most effective when a helical field has largely lifted off the photosphere into the chromosphere producing the large-scale streaming along active region filaments often seen in this higher part of the atmosphere (Martin, 1989; Zirin 1988).

The lifting of the bottom of a closed magnetic field from the photosphere has a characteristic signature. As the bottom leaves the photosphere, the bipolar magnetic patches corresponding to the intersection of a flux bundle with the photosphere will appear to converge and mutually annihilate. Moreover, the annihilation is clean and complete to the extent that the entire flux bundle lifts above the photosphere.

Clean cancellation of opposite magnetic patches have been observed on the photosphere in magnetic data, ranging from dipoles associated with X-ray bright points, through sunspot-like bipolar polarities, to small active regions (Harvey, Harvey, and Martin, 1975; Harvey and Martin, 1973; Rabin, Moore, and Hagyard, 1984; Spruit, Title, and van Ballegooijen, 1987; Webb *et al.*, 1993; Zirin, 1985). A popular interpretation of these observations is the submergence of magnetic flux. From our analysis here, it seems more likely that these observed events indicate flux *emergence* of 'U' loops through the photosphere. Martin (1989) reported that the formation of a prominence is accompanied with the systematic drifts of magnetic elements (of the opposite signs) coming from the two sides of the polarity inversion line to meet and cancel. The systematic lifting off of 'U' loops from the photosphere and low chromosphere as the result of the rise of a horizontal flux rope, with a quiescent prominence forming in it, would explain this observation. Finally, the magnetic field along the polarity inversion line in this process would be concaved upward, consistent with the prominence in the inverse configuration, and, more recently, supported by direct vector field measurements (Lites *et al.*, 1995).

Theoretically, the buoyant rise of a U loop is a simple geometric explanation of why, at the photosphere, two magnetic elements of the opposite polarities should seek each other out to annihilate. On the contrary, if two photospheric patches of opposite polarities are connected by the traditional, bipolar (inverted 'U') loop in the atmosphere above, it is unlikely to have the tenuous atmosphere above force the entire magnetic field back down to submerge it below the photosphere. Another case to consider is one where the two photospheric magnetic patches are not magnetically connected. Then special photospheric flows have to be invoked to explain why the two patches come together. Such flows are not readily justified since the photosphere is sufficiently massive to advect its embedded fields along, with no physical need to bring opposite fields into contact. Moreover, if two unconnected opposite fields are brought by the flows to reconnect, the reconnection generally takes place at a neutral sheet lying up in the tenuous atmosphere and therefore does not produce a flux cancellation at the photosphere (Golub *et al.*, 1981). It takes a stipulation of artificial conditions to have the reconnection occur at a neutral point right in the photosphere to produce polarity cancellation at the photosphere.

In contrast, a rising 'U' loop explains the clean polarity cancellation, first at the photosphere and later at the higher levels of the atmosphere.

There is another, different, way for a magnetic flux rope to form in the corona. As the magnetic fields of all scales emerge in an active region and interact with one another, they coalesce and flare away their small-scale structures to form a more ordered large-scale structure. If the coalescing structures are of random signs in magnetic helicity, the resultant large-scale structure may end up in a near-potential state with a negligible total helicity. It then takes the form of an untwisted bipolar magnetic structure with no significant stored energy. If the coalescing structures are all of the same sign in magnetic helicity, the resultant large-scale structure by some suitable form of the conservation of helicity would inherit a considerable sum of all the helicities contributed by the different parts. The resultant large-scale magnetic structure is then significantly twisted as in the case of a major magnetic flux rope. In this case, the flux rope forms in the corona without necessarily involving any observable flux rope passing through the photosphere in a coherent form, such as we have interpreted in the case of a delta-sunspot.

Whether the coalescing structures are of the same sign in helicity is a fundamental factor in this process. On the Sun, there is a definite hemispherical preference of helicity of a fixed sign, negative and positive, respectively, in the northern and southern hemispheres, as we have pointed out in the discussion on prominences. We therefore conclude that an end product of an active region is a magnetic flux rope of considerable amount of accumulated flux and magnetic helicity, emphasizing that the latter is made up of contributions largely of the same sign in a given hemisphere. This flux rope may be identified with the cavity of a well formed high latitude crown filament. Such a filament and its cavity is very stable, as observed, for it is the end-product of a tortuous path of the total system via successive flaring episodes towards an energy minimum state. It is the approximate conservation of magnetic helicity which retains a certain finite amount of magnetic energy in that minimum-energy state and prevent it from being flared away.

If the solar dynamo and the emergence of flux are artificially switched off and the anchored part of the magnetic fields remain rigidly rooted to the photosphere, the helmet streamer belts would remain permanently in the corona by virtue of their stability and the extremely long electrical resistive time scale associated with the million-degree temperature. The dynamo of course continues to drive with its eleven-year cycle in its usual operation. As sketched in Figure 3(a), the prominence flux rope needs to be held down by the anchored bipolar field of the helmet dome. These bipolar fields could actually be a part of the global flux rope with their feet connected topologically below the base of the corona (not shown in Figure 3(b)) to close around the coronal cavity. As the bottoms of these closed fields lift into the corona in the general emergence process, there is, in the corona, a conversion of anchored flux to detached flux. The flux rope rises and stretches the diminishing amount of anchoring flux. Eventually, the quasi-steadily growing flux rope cannot be held down in equilibrium. It breaks away and a CME is initiated, to eject, as

we now recognize, not just the enormous mass of the helmet dome, but also the accumulated magnetic flux and helicity in the flux rope.

It is at this step of our synthesis that we see a clear role for the CME in the global process of solar activity. As a mass loss mechanism, the CME is not significant compared to the more or less steady solar wind. It is far more important as a means of ejection of magnetic flux and helicity which by virtue of the high electrical conductivity would otherwise progressively accumulate in the corona. Such an accumulation clearly cannot take place beyond eleven years, when the entire atmospheric magnetic field is rebuilt, with the opposite polarity, from new-cycle fields coming up from the convection zone. The helmet structure and its cavity store the old flux and helicity in the corona and the CME takes them away largely as an ideal MHD process with no significant heating of the corona (Hiei, Hundhausen, and Sime, 1994; Low, 1994a).

The active region does not expel its magnetic flux and helicity all in one final event. Whenever a flux rope is unable to hold itself down, a CME takes off with the flux rope. The opened field reconnects to produce the flare. This may occur in an active region long before the active region begins to decay. Such CMEs are associated with post-CME flares which are highly energetic and complicated because the latter involve the intense ( $> 100$  G) and contorted fields of a mature active region (Hundhausen, 1995b).

The reclosing of opened magnetic fields after a CME has been observed to reform a helmet streamer (Hiei, Hundhausen, and Sime, 1994). It seems plausible that subsequent flux emergence into the corona results in the formation of a cavity in the interior of the reformed helmet, with or without a prominence reforming within the cavity. This then sets the stage for another CME. This process may therefore repeat several times until no more flux emerges to form the coronal cavity, which we recall is the principal mechanism for storing energy for a CME eruption. It should be noted that the rise of 'U' loops from the coronal base to form the cavity flux rope naturally reduces the amount of flux threading through the coronal base by the cancellation of equal amounts of fluxes of the opposite signs. This process is therefore a promising candidate for the removal of the magnetic flux through the base of the corona, which we know must take place systematically to change the magnetic polarity of the entire corona at the end of each solar cycle. We have not proven that this process of repeated CMEs takes place in the corona although the observations we have reviewed are, in many respects, consistent with it. We suggest that this process merits further theoretical and observational investigation.

## 5. Summary and Conclusion

The qualitative physical picture we have synthesized delineates a chain of relationships linking together various solar MHD phenomena, including, in particular, prominences, heating, flares, helmet streamers, and CMEs. These relationships

point to a global view of the corona as a plasma system responding dynamically to the injection of magnetic flux in the course of a dynamo cycle.

The central stage is taken by the structures formed out of the emerged flux. These structures are characterized with a certain long-lived identity, days to weeks, as they evolve quasi-steadily, driven by photospheric motion and by further flux emergence. At every opportunity permitted by the relevant dynamical constraints, such a structure breaks from its quiescence to liberate energy in order to relax once again to another stable quiescent state. The break is due either to an internal build-up of stress or to interaction with other structures. The amounts of energy liberated form a continuous spectrum, ranging from the quiescent heating of the corona with little large-scale change in the magnetic field to the violence of a major flare or the CME.

Our physical picture became clear only recently as the result of both theoretical and observational developments. There are three major developments, summarized below, which filled in several important gaps in our understanding and made our synthesis, at least, conceptually complete. All three developments lead independently to the suggestion that magnetic flux ropes form commonly in the corona as the result of flux emergence. These flux ropes manifest as the filament channels in the chromosphere and low-density cavities in the corona.

The first development is the unraveling of the CME-flare relationship (Harrison, 1986, 1991; Hundhausen, 1988, 1995b) and the proposal that the helmet cavity as a magnetic flux rope may provide the means of storing energy for the CME-flare process (Low and Smith, 1993). In the latter concern, the conjecture of Aly (1984, 1991) that there is a limit on the free energy of force-free magnetic fields is an important conceptual step towards recognizing the importance of pressure and gravity for phenomena involving the large scales in the corona.

The second development has its beginning in flare studies using vector magnetograms over the years. The simple-minded expectation was often not met that a flare should take a stressed magnetic field via current dissipation to a less-sheared potential-like configuration (Hagyard and Rabin, 1986). There is an accumulation of observational evidence over the years that magnetic fields commonly emerge with a significant twist. Moreover, it has been well known that a prominence usually forms after a flux-emergence flare in an active region. These phenomena fit the expectation, as an extension of Taylor's postulate, that flaring regarded as a reconnection process in a medium of high magnetic Reynolds number cannot get rid of the global twist of the solar magnetic field. The preserved twist retains a considerable amount of energy in the relaxed magnetic field. The discovery that most prominences are of the inverse polarity configuration (Foukal, 1971; Leroy, 1989; Martin *et al.*, 1993) and the successful modeling of this configuration in terms of the prominence in a cavity flux rope (Low and Hundhausen, 1995) led us to suggest that the cavity flux rope is where the preserved magnetic twist resides in the post-flare quiescent state.

The third development is the discovery of the hemispherical preferences for a fixed sign of magnetic helicity or handedness of magnetic twist (Leroy, 1989; Martin *et al.*, 1993; Pevtsov, Canfield, and Metcalf, 1994, 1995; Rust, 1994; Richardson, 1941). This has the implication that magnetic structures in the same hemisphere generally have the same handedness in twist. Given that the global twists combine additively, it follows that magnetic helicity by some suitable measure would accumulate in the corona. Yet the corona must completely reverse its global field at the end of each eleven-year solar cycle. Since the accumulated magnetic twist resides in the cavity flux rope, in our interpretation, it then follows that the CMEs are the means by which the accumulated magnetic flux and twist are taken out of the corona.

It is interesting that the stages of evolution of a coronal structure from its first emergence in the solar atmosphere to being thrown out of the corona may be understood qualitatively in terms of a complementary interplay among resistive MHD turbulence, ideal ordered MHD flows, and magnetic helicity. Coronal heating, flares and CMEs do not occur arbitrarily in the structure's history but is related by these basic processes to specific stages of the structure's evolution. It is these relationships that give physical meaning to the classification of flares in Section 4.2.

This review is an attempt to provide a comprehensive basis for our physical picture. It should also be pointed out that many important solar phenomena not related to the central physical questions of our concerns have been left out. The appeal of our physical picture is its simplicity and clear articulation of what physics we are talking about. We have provided only a qualitative discussion of the basic physics. Much work, theoretical and observational, needs to be done to further develop and test the ideas. It should not be a surprise that future quantitative formulations of these ideas show subtle physics not accounted for in our broad-brush approach and new constructions and modifications are needed to get the physics right and to agree with observation. On the other hand, the way the different pieces of observations and theoretical ideas are fitting in with each other suggests that our physical picture is qualitatively in the right direction.

### Acknowledgements

I wish to thank many colleagues who over time have helped me greatly in my effort to understand both theory and observations, notably, Peter Gilman, Art Hundhausen, Bruce Lites, Sara Martin, Gene Parker, Valentin Martinez Pillet, Andy Skumanich, and Rich Wolfson. I also wish to thank Art for sharing his insights in coronal observation and interpretation, Peter for critically reviewing an earlier draft, Liz Boyd for preparing this manuscript, and Joan Burkepile for preparing several figures.

## References

- Aly, J. J.: 1984, *Astrophys. J.* **283**, 349.  
 Aly, J. J.: 1991, *Astrophys. J.* **375**, L61.  
 Aly, J. J.: 1992, *Solar Phys.* **138**, 133.  
 Amari, T.: 1990, in E. R. Priest (ed.), *Advances in Solar System Magnetohydrodynamics*, D. Reidel Publ., Dordrecht, Holland, p. 3.  
 Antiochos, S. K., Dahlburg, R. B., and Klimchuk, J. A.: 1994, *Astrophys. J.* **420**, L41.  
 Anzer, U.: 1989, in E. R. Priest (ed.), *Dynamics and Structures of Quiescent Solar Prominences*, D. Reidel Publ. Co., Dordrecht, Holland, p. 143.  
 Athay, R. G.: 1988, in F. A. Cardova (ed.), *Multiwavelength Astrophysics*, Cambridge University Press, Cambridge, p. 7.  
 Athay, R. G., Jones, H. P., and Zirin, H.: 1985a, *Astrophys. J.* **288**, 363.  
 Athay, R. G., Jones, H. P., and Zirin, H.: 1985b, *Astrophys. J.* **291**, 344.  
 Athay, R. G., Querfeld, C. W., Smartt, R. N., Landi degl'Innocenti, E., and Bommier, V.: 1983, *Solar Phys.* **89**, 3.  
 Barnes, C. W. and Sturrock, P. A.: 1972, *Astrophys. J.* **174**, 659.  
 Berger, M. A.: 1984, *Geophys. Astrophys. Fluid Dyn.* **30**, 79.  
 Berger, M. A.: 1985, *Astrophys. J. Suppl.* **59**, 433.  
 Berger, M. and Field, G.: 1986, *J. Fluid Mech.* **147**, 133.  
 Billings, D. E.: 1966, *A Guide to the Solar Corona*, Academic Press, New York.  
 Bogdan, T. and Duval, T. L., Jr.: 1996, preprint.  
 Canfield, R., Priest, E. R., and Rust, D. M.: 1974, Y. Nakagawa and D. M. Rust (eds.), *Flare-Related Magnetic Field Dynamics*, NCAR, p. 361.  
 Cargill, P.: 1993, in J. L. Birch and J. H. Waite (eds.), *Solar System Plasma Physics: Resolution of Processes in Space and Time*, AGU Publication.  
 Choe, G. S. and Lee, L. C.: 1992, *Solar Phys.* **138**, 291.  
 Chou, Y. P. and Low, B. C.: 1994, *Solar Phys.* **153**, 255.  
 Choudhuri, A. R. and Gilman, P. A.: 1987, *Astrophys. J.* **316**, 788.  
 Crito, F., Picat, J. P., and Cailloux, M.: 1983, *Solar Phys.* **83**, 143.  
 de La Beajardière, J. F., Canfield, R. C., Hudson, H. S., Wülser, J.-P., Acton, L., Kosugi, T., and Masuda, S.: 1995, *Astrophys. J.* **440**, 386.  
 Démoulin, P. and Forbes, T. G.: 1992, *Astrophys. J.* **387**, 394.  
 Démoulin, P., Hénoux, J. C., and Mandrini, C. H.: 1992, *Solar Phys.* **139**, 105.  
 Dodson, H. W. and Hedeman, E. R.: 1970, *Solar Phys.* **13**, 401.  
 Dombre, T., Frisch, U., Greene, J. M., Hénon, M., Mehr, A., and Soward, A. M.: 1986, *J. Fluid Mech.* **16**, 353.  
 Dryer, M.: 1982, *Space Sci. Rev.* **33**, 233.  
 Dryer, M. and Wu, S. T.: 1985, *J. Geophys. Res.* **90**, 559.  
 D'Silva, S.: 1995, *Astrophys. J.* **448**, 459.  
 Duvall, T. L., Jr., Jefferies, S. M., Harvey, J. W., Schou, J., and D'Silva, S.: 1996, preprint.  
 Eddy, J. A.: 1978, in J. A. Eddy (ed.), *The New Solar Physics*, Westview Press, Boulder, p. 11.  
 Engvold, O.: 1989, in E. R. Priest (ed.), *Dynamics and Structures of Quiescent Prominences*, D. Reidel Publ. Co., Dordrecht, Holland, p. 47.  
 Fan, Y., Fisher, G. H., and DeLuca, E. E.: 1993, *Astrophys. J.* **405**, 390.  
 Ferriz-Mas, A. and Schüssler, M.: 1993, *G.A.F.D.* **72**, 209.  
 Finn, J. M.: 1986, *Phys. Fluids* **29**, 2630.  
 Fisher, R. R.: 1984, *Adv. Space Res.* **4**, 163.  
 Fisher, R. R. and Poland, A. I.: 1981, *Astrophys. J.* **246**, 1004.  
 Fisher, R. R., Garcia, C. J., and Seagraves, P.: 1981, *Astrophys. J.* **246**, L161.  
 Forbes, T. G.: 1992, in Z. Švestka, B. V. Jackson, and M. E. Machado (eds.), *Eruptive Solar Flares*, Kluwer Academic Publishers, Dordrecht, Holland, p. 79.  
 Forbes, T. G. and Malherbe, J. M.: 1986, *Astrophys. J.* **302**, L67.  
 Foukal, P.: 1971, *Solar Phys.* **19**, 59.  
 Gaizauskas, V., Harvey, K. L., Harvey, J. W., and Zwaan, C.: 1983, *Astrophys. J.* **256**, 1056.

- Gilman, P. A.: 1986, in P. A. Sturrock, T. E. Holzer, D. M. Mihalas, and R. K. Ulrich (eds.), *Physics of the Sun*, D. Reidel Publ. Co., Dordrecht, Holland, Vol. 1, Ch. 5.
- Gold, T.: 1964, in W. N. Hess (ed.), *Physics of Solar Flares*, NASA, Washington, DC, p. 389.
- Golub, L., Rosner, R., Vaiana, G. S., and Weiss, N. O.: 1981, *Astrophys. J.* **243**, 309.
- Gosling, J. T.: 1993a, *J. Geophys. Res.* **98**, 18937.
- Gosling, J. T.: 1993b, *Phys. Fluids* **B5**, 2638.
- Gosling, J., Bame, S. J., McComas, D. J., Phillips, J. L., Goldstein, B. E., and Neugebaur, M.: 1994, *Geophys. Res. Letters* **21**, 1109.
- Gosling, J. T., Hildner, E., MacQueen, R. M., Munro, R. H., Poland, A. I., and Ross, C. L.: 1976, *Solar Phys.* **48**, 389.
- Guhathakurta, M. and Fisher, R. R.: 1994, *Solar Phys.* **152**, 181.
- Habbal, S. R.: 1992, *Ann. Geophys.* **10**, 34.
- Hagyard, M. J. and Rabin, D. M.: 1986, *Adv. Space Res.* **6**, 7.
- Harrison, R. A.: 1986, *Astron. Astrophys.* **162**, 283.
- Harrison, R. A.: 1991, *Adv. Space Res.* **11**, 25.
- Harvey, K. L., and Martin, S. F.: 1973, *Solar Phys.* **32**, 389.
- Harvey, K. L., Harvey, J. W., and Martin, S. F.: 1975, *Solar Phys.* **40**, 87.
- Heinemann, M. and Olbert, S.: 1978, *J. Geophys. Res.* **83**, 2457.
- Heyvaert, J. and Priest, E. R.: 1984, *Astron. Astrophys.* **137**, 63.
- Hiei, E., Hundhausen, A. J., and Sime, D. G.: 1994, *Geophys. Res. Letter* **20**, 2785.
- Hildner, E.: 1992, in Z. Švestka, B. V. Jackson, and M. E. Machado (eds.), *Eruptive Solar Flares*, Springer-Verlag, Berlin, p. 227.
- Hirayama, T.: 1974, *Solar Phys.* **34**, 389.
- Hollweg, J. V.: 1991, in P. Ulmschneider, E. R. Priest, and R. Rosner (eds.), *Mechanisms of Chromospheric and Coronal Heating*, Springer-Verlag, Berlin, p. 423.
- House, L. L. and Smartt, R. N.: 1982, *Solar Phys.* **80**, 53.
- Howard, R.: 1972, *Solar Phys.* **25**, 5.
- Howard, R. A., Sheely, N. R., Jr., Koomen, M. J., and Michels, D. J.: 1985, *J. Geophys. Res.* **90**, 8173.
- Howard, R. A., Sheely, N. R., Jr., Michels, D. J., and Koomen, M. J.: 1986, in R. G. Marsden (ed.), *The Sun and the Heliosphere in Three Dimensions*, D. Reidel Publ. Co., Dordrecht, Holland, p. 107.
- Hu, Y. Q. and Low, B. C.: 1989, *Astrophys. J.* **342**, 1049.
- Hu, Y. Q., Zhu, Z., Hundhausen, A. J., Holzer, T. E., and Low, B. C.: 1990, *Sci. Sinica* **333**, 332.
- Hudson, H. S.: 1991, *Solar Phys.* **133**, 357.
- Hundhausen, A. J.: 1972, *Coronal Expansion and Solar Wind*, Springer-Verlag, New York.
- Hundhausen, A. J.: 1977, in J. B. Zirker (ed.), *Coronal Holes and High Speed Wind Streams*, Colorado Associated University Press, Boulder CO, p. 225.
- Hundhausen, A. J.: 1988, in V. Pizzo, D. G. Sime, and T. E. Holzer (eds.), *Proc. Sixth International Solar Wind Conference*, NCAR TN-306, Vol. 1, Boulder, CO, p. 181.
- Hundhausen, A. J.: 1993, *J. Geophys. Res.* **98**, 13177.
- Hundhausen, A. J.: 1994, in M. G. Kivelson and C. T. Russell (eds.), *Introduction to Space Physics*, Cambridge University Press, Cambridge.
- Hundhausen, A. J.: 1995a, private communication.
- Hundhausen, A. J.: 1995b, in K. Strong, J. Saba, and B. Haisch (eds.), *The Many Faces of the Sun*, in press.
- Hundhausen, A. J., Burkepile, J. T., and St. Cyr, O. C.: 1994, *J. Geophys. Res.* **99**, 6543.
- Hundhausen, A. J., Holzer, T. E., and Low, B. C.: 1987, *J. Geophys. Res.* **92**, 11173.
- Hundhausen, J. R., Hundhausen, A. J., and Zweibel, E. G.: 1981, *J. Geophys. Res.* **86**, 11117.
- Hundhausen, A. J., Stanger, A. L., and Serbicki, S. A.: 1994, *Proc. 3rd SOHO Workshop*, European Space Agency, Paris, p. 409.
- Hundhausen, A. J. and 14 co-authors: 1984, in D. M. Butler and K. Papadopoulos (eds.), *Solar Terrestrial Physics, Present and Future*, NASA Ref. Publ. No. 1120 Washington, D.C.
- Illing, R. M. E.: 1984, *Astrophys. J.* **280**, 399.
- Illing, R. M. E. and Hundhausen, A. J.: 1985, *J. Geophys. Res.* **90**, 275.

- Illing, R. M. E. and Hundhausen, A. J.: 1986, *J. Geophys. Res.* **91**, 10951.
- Inhester, B., Birn, J., and Hesse, M.: 1992, *Solar Phys.* **138**, 257.
- Jansen, T. and Chu, M.: 1984, *Phys. Fluids* **27**, 2881.
- Kahler, S.: 1992, *Ann. Rev. Astron. Astrophys.* **30**, 113.
- Klimchuk, J. A.: 1990, *Astrophys. J.* **354**, 745.
- Kopp, R. and Pneuman, G. W.: 1976, *Solar Phys.* **50**, 85.
- Kurokawa, H.: 1987, *Solar Phys.* **113**, 259.
- Kusano, K., Suzuki, Y., and Nishikawa, K.: 1995, *Astrophys. J.* **441**, 942.
- Laurence, P. and Avellaneda, M.: 1993, *Geophys. Astrophys. Fluid Dyn.* **69**, 201.
- Leka, K. D., Canfield, R. C., McClymont, A. N., and van Driel-Gésztesy, L.: 1996, *Astrophys. J.*, in press.
- Leroy, J. L.: 1989, in E. R. Priest (ed.), *Dynamics and Structures of Quiescent Solar Prominences*, Kluwer Academic Publishers, Dordrecht, Holland, p. 77.
- Leroy, J. L., Bommier, V., and Sahal-Bréchot, S.: 1983, *Solar Phys.* **83**, 135.
- Leroy, J. L., Bommier, V., and Sahal-Bréchot, S.: 1984, *Astron. Astrophys.* **131**, 33.
- Lites, B. W., Low, B. C., Martinez-Pillet, V., Seagraves, P., Skumanich, A., Frank, Z. A., Shine, R. A., and Tsuneta, S.: 1995, *Astrophys. J.* **446**, 877.
- Livi, S. H. B., Martin, S. F., Wang, H., and Ai, G.: 1989, *Solar Phys.* **121**, 197.
- Low, B. C.: 1980, *Solar Phys.* **65**, 147.
- Low, B. C.: 1981, *Astrophys. J.* **251**, 352.
- Low, B. C.: 1982a, *Rev. Geophys. Space Phys.* **20**, 145.
- Low, B. C.: 1982b, *Astrophys. J.* **254**, 796.
- Low, B. C.: 1984, *Astrophys. J.* **281**, 392.
- Low, B. C.: 1985, *Solar Phys.* **100**, 309.
- Low, B. C.: 1986, *Astrophys. J.* **307**, 205.
- Low, B. C.: 1989, *Astrophys. J.* **340**, 558.
- Low, B. C.: 1990, *Ann. Rev. Astron. Astrophys.* **28**, 491.
- Low, B. C.: 1993a, *Astrophys. J.* **409**, 798.
- Low, B. C.: 1993b, *Adv. Space Res.* **13**, 63.
- Low, B. C.: 1993c, *Bull. Astron. Astrophys. Soc.* **25**, 1218.
- Low, B. C.: 1994a, *Plasma Phys.* **1**, 1684.
- Low, B. C.: 1994b, in *Third SOHO Workshop: Solar Dynamic Phenomena and Solar Wind Consequences*, European Space Agency, Paris, p. 123.
- Low, B. C. and Hundhausen, A. J.: 1987, *J. Geophys. Res.* **92**, 2221.
- Low, B. C. and Hundhausen, J. R.: 1995, *Astrophys. J.* **443**, 818.
- Low, B. C. and Lou, Y. Q.: 1990, *Astrophys. J.* **352**, 343.
- Low, B. C. and Smith, D. F.: 1993, *Astrophys. J.* **410**, 413.
- Low, B. C. and Wolfson, R.: 1988, *Astrophys. J.* **324**, 574.
- Low, B. C., Munro, R. H., and Fisher, R. R.: 1982, *Astrophys. J.* **254**, 335.
- Lu, E. and Hamilton, R.J.: 1991, *Astrophys. J.* **380**, L89.
- Lu, E. Hamilton, R. J., McTiernan, J. M., and Bromund, K.: 1993, *Astrophys. J.* **412**, 841.
- MacQueen, R. M.: 1980, *Phil. Trans. Roy. Soc. London A* **297**, 605.
- Martin, S. F.: 1980, *Solar Phys.* **68**, 217.
- Martin, S. F.: 1989, in V. Ruždjak and E. Tandberg-Hanssen (eds.), *Dynamics of Quiescent Prominences*, Springer-Verlag, Berlin, p. 1.
- Martin, S. F. and McAllister, A.: 1995, in *Proc. IAU Colloq. 153*.
- Martin, S. F., Bilimoria, R., and Tracadas, P. W.: 1993, in R.J. Rutten and C.J. Schrijver (eds.), *Solar Surface Magnetism*, Kluwer Academic Publishers, Dordrecht, Holland, p. 303.
- Mason, S. F. and Bassey, R. J.: 1983, *Solar Phys.* **83**, 121.
- Masuda, S., Kosugi, T., Hara, H., Tsuneta, S., and Ogawara, Y.: 1994, *Nature* **371**, 495.
- Matsumoto, R., Tajima, T., Shibata, K., and Kaisig, M.: 1993, *Astrophys. J.* **414**, 357.
- Matthews, P. C., Hughes, D. W., and Proctor, M. R. E.: 1995, *Astrophys. J.* **448**, 938.
- McIntosh, P. S.: 1972, *Prog. Astronaut. Aeronaut.* **30**, 65.
- Metcalf, T. R., Jiao, L., McClymont, A. N., and Canfield, R. C.: 1995, *Astrophys. J.* **437**, 474.
- Mikić, Z. and Linker, J. A.: 1994, *Astrophys. J.* **430**, 898.

- Moffatt, H. K.: 1978, *Magnetic Field Generation in Electrically Conducting Fluids*, Cambridge University Press, New York.
- Moore, R. L., Hurford, G. J., Jones, H. P., and Kane, S. R.: 1984, *Astrophys. J.* **276**, 379.
- Moreno-Insertis, F.: 1992, in J. H. Thomas and N. O. Weiss (eds.), *Sunspots, Theory, and Observations*, Kluwer Academic Publishers, Dordrecht, Holland, p. 385.
- Mouschovias, T. Ch.: 1974, *Astrophys. J.* **192**, 37.
- Munro, R. H., Gosling, J. T., Hildner, E., MacQueen, R. M., Poland, A. I., and Ross, C. L.: 1979, *Solar Phys.* **61**, 201.
- Norman, C. A. and Heyvaerts, J.: 1983, *Astron. Astrophys.* **124**, L1.
- Ogawara, Y., Acton, L. W., Bentley, R. D., Bruner, M. E., Culhane, J. L., Hiei, E., Hirayama, T., Hudson, H. S., Kosugi, T., Lemen, J. R., Strong, K. T., Tsuneta, S., Uchida, Y., Watanabe, T., and Yoshimori, M.: 1992, *Publ. Astron. Soc. Japan* **44**, L41.
- Pap, J., Fröhlich, C., Hudson, H., and Tobiska, W. K. (eds.): 1994, *Solar Phys.* **152**.
- Parker, E. N.: 1955, *Astrophys. J.* **121**, 491.
- Parker, E. N.: 1963, *Interplanetary Dynamical Processes*, Interscience, New York.
- Parker, E. N.: 1966, *Astrophys. J.* **145**, 811.
- Parker, E. N.: 1975, *Astrophys. J.* **202**, 523.
- Parker, E. N.: 1977, *Ann. Rev. Astron. Astrophys.* **15**, 45.
- Parker, E. N.: 1979, *Cosmical Magnetic Fields*, Oxford University Press, Oxford.
- Parker, E. N.: 1984, *Astrophys. J.* **280**, 423.
- Parker, E. N.: 1987, *Solar Phys.* **110**, 11.
- Parker, E. N.: 1988, *Astrophys. J.* **330**, 474.
- Parker, E. N.: 1989, *Geophys. Astrophys. Fluid Dyn.* **45**, 159.
- Parker, E. N.: 1994a, *Spontaneous Current Sheets in Magnetic Fields*, Cambridge University Press, Cambridge.
- Parker, E. N.: 1994b, *Astrophys. J.* **433**, 867.
- Parker, E. N.: 1995a, *Astrophys. J.* **440**, 415.
- Parker, E. N.: 1995b, *Astrophys. J.* **442**, 405.
- Parker, E. N.: 1995c, *Astrophys. J.* **448**, 942.
- Pevtsov, A. A., Canfield, R. C., and Metcalf, T. R.: 1994, *Astrophys. J.* **425**, L117.
- Pevtsov, A. A., Canfield, R. C., and Metcalf, T. R.: 1995, *Astrophys. J.* **440**, L109.
- Pneuman, G. W.: 1972, *Astrophys. J.* **177**, 793.
- Pneuman, G. W.: 1983, *Solar Phys.* **88**, 219.
- Pneuman, G. W. and Kopp, R. A.: 1971, *Solar Phys.* **18**, 258.
- Poland, A. I. and MacQueen, R. M.: 1981, *Solar Phys.* **71**, 361.
- Poland, A. I. and Mariska, J. T.: 1986, *Solar Phys.* **104**, 303.
- Priest, E. R.: 1982, *Solar Magnetohydrodynamics* D. Reidel Publ. Co., Dordrecht, Holland.
- Priest, E. R. (ed.): 1989, *Dynamics and Structure of Solar Prominences*, Kluwer Academic Publishers, Dordrecht, Holland.
- Priest, E. R., Hood, A. W., and Anzer, U.: 1989, *Astrophys. J.* **344**, 1010.
- Rabin, D., Moore, R. L., and Hagyard, M. J.: 1984, *Astrophys. J.* **287**, 404.
- Radick, R., Lockwood, G. W., and Baliunas: 1990, *Science* **247**, 39.
- Richardson, R. S.: 1941, *Astrophys. J.* **93**, 24.
- Ridgeway, C. and Priest, E. R.: 1993, *Solar Phys.* **146**, 277.
- Roumeliotis, G., Sturrock, P. A., and Antiochos, S. K.: 1994, *Astrophys. J.* **423**, 847.
- Rust, D. M.: 1967, *Astrophys. J.* **150**, 313.
- Rust, D. M.: 1976, *Solar Phys.* **47**, 21.
- Rust, D.: 1994, *Geophys. Res. Letters* **21**, 241.
- Rust, D. M. and Kumar, P.: 1994, *Solar Phys.* **155**, 69.
- Saito, K. and Hyder, C.: 1968, *Solar Phys.* **5**, 61.
- Saito, K. and Tandberg-Hanssen, E.: 1973, *Solar Phys.* **31**, 105.
- Sakurai, T.: 1985, *Astron. Astrophys.* **152**, 121.
- Sakurai, T.: 1989, *Space Sci. Rev.* **51**, 11.
- Schönenfelder, A. O. and Hood, A.: 1995, *Solar Phys.* **157**, 223.
- Schüssler M.: 1979, *Astron. Astrophys.* **71**, 79.

- Seehafer, N.: 1978, *Solar Phys.* **58**, 215.  
 Seehafer, N.: 1990, *Solar Phys.* **125**, 219.  
 Serio, S., Vaiana, G. S., Godoli, G., Motta, S., Pirronello, V., and Zappaloa, R. A.: 1978, *Solar Phys.* **59**, 65.  
 Shea, M. A. (ed.): 1991, *Contributions in Solar-Planetary Relationships*, U.S. National Report: 1987 – 1990, suppl. to *Rev. Geophys.*, AGU, Washington DC.  
 Sheeley, N. R., Jr., Howard, R. A., Koomen, M. J., and Michels, D. J.: 1983, *Astrophys. J.* **272**, 349.  
 Sheeley, N. R., Jr., Howard, R. A., Koomen, M. J., Michels, D. J., Schwenn, R., Mühlhauser, K. H., and Rosenbauer, H.: 1985, *J. Geophys. Res.* **90**, 163.  
 Shi, Z. and Wang, J.: 1994, *Solar Phys.* **149**, 105.  
 Shibata, K., Nozawa, S., Matsumoto, R., Sterling, A. C., and Tajima, T.: 1990, *Astrophys. J.* **351**, L25.  
 Sime, D. G.: 1989, *J. Geophys. Res.* **94**, 151.  
 Sime, D. G. and Hundhausen, A. J.: 1987, *J. Geophys. Res.* **92**, 1049.  
 Sime, D. G., MacQueen, R. M., and Hundhausen, A. J.: 1984, *J. Geophys. Res.* **89**, 2113.  
 Sime, D. G., MacQueen, R. M., and Hundhausen, A. J.: 1985, *J. Geophys. Res.* **90**, 563.  
 Smith, E. A. and Priest, E. R.: 1977, *Solar Phys.* **53**, 25.  
 Spruit, H. C., Title, A. M., and van Ballegooijen, A. A.: 1987, *Solar Phys.* **110**, 115.  
 Steiner, O., Knoelker, M., and Schüssler, M.: 1994, in R. J. Rutten and C. J. Schrijver (eds.), *Solar Surface Magnetism*, Kluwer Academic Publishers, Dordrecht, Holland, p. 441.  
 Steinolfson, R.: 1988, *J. Geophys. Res.* **93**, 14261.  
 Steinolfson, R. S.: 1991, *Astrophys. J.* **382**, 677.  
 Steinolfson, R. S. and Hundhausen, A. J.: 1989, *J. Geophys. Res.* **94**, 1222.  
 Steinolfson, R. S. and Hundhausen, A. J.: 1990, *J. Geophys. Res.* **95**, 20693.  
 Steinolfson, R., Suess, S. T., and Wu, S. T.: 1982, *Astrophys. J.* **255**, 730.  
 Stenflo, J.: 1994, *Solar Magnetic Fields*, Kluwer Academic Publishers, Dordrecht, Holland.  
 Sturrock, P. A.: 1991, *Astrophys. J.* **380**, 655.  
 Švestka, Z.: 1976, *Solar Flares*, D. Reidel Publ. Co., Dordrecht, Holland.  
 Tanaka, K.: 1991, *Solar Phys.* **136**, 133.  
 Tandberg-Hanssen, E.: 1974, *Solar Prominences*, D. Reidel Publ. Co., Dordrecht, Holland.  
 Tandberg-Hanssen, E.: 1995, *Solar Prominences*, Kluwer Academic Publishers, Dordrecht, Holland.  
 Tang, F.: 1985, *Solar Phys.* **102**, 131.  
 Tang, F.: 1987, *Solar Phys.* **107**, 233.  
 Taylor, J. B.: 1974, *Phys. Rev. Letters* **33**, 1139.  
 Taylor, J. B.: 1986, *Rev. Mod. Phys.* **58**, 741.  
 Thomas, J. H. and Weiss, N. O. (eds.): 1991, *Sunspots, Theory and Observations*, Kluwer Academic Publishers, Dordrecht, Holland.  
 Tsinganos, K. and Low, B. C.: 1989, *Astrophys. J.* **342**, 1028.  
 Tsuneta, S.: 1996a, *Astrophys. J.*, in press.  
 Tsuneta, S.: 1996b, *Astrophys. J.*, in press.  
 Tsuneta, S., Hara, H., Shimizu, T., Acton, L. W., Strong, K. T., Hudson, H., and Ogawara, Y.: 1992, *Publ. Astron. Soc. Japan* **44**, L63.  
 Uchida, Y. and Low, B. C.: 1982, *J. Astron. Astrophys.* **2**, 405.  
 van Ballegooijen, A. A. and Martens, P. C. H.: 1989, *Astrophys. J.* **343**, 971.  
 van Ballegooijen, A. A. and Martens, P. C. H.: 1990, *Astrophys. J.* **361**, 283.  
 Vekstein, G. E., Priest, E. R., and Steele, C. D.: 1991, *Solar Phys.* **131**, 297.  
 Vrsnak, B., Rudžjak, V., and Rompolt, B.: 1991, *Solar Phys.* **136**, 151.  
 Wang, H.: 1992, *Solar Phys.* **140**, 85.  
 Wang, J.: 1994, *Solar Phys.* **155**, 285.  
 Wang, H. and Tang, F.: 1993, *Astrophys. J.* **407**, L89.  
 Wang, H., Ewell, M. W., Jr., Zirin, H., and Ai, G.: 1994, *Astrophys. J.* **424**, 436.  
 Webb, D. F. and Howard, R. A.: 1994, *J. Geophys. Res.* **99**, 4201.  
 Webb, D. F. and Hundhausen, A. J.: 1987, *Solar Phys.* **108**, 383.  
 Webb, D. F., Martin, S. F., Moses, D., and Harvey, J. W.: 1993, *Solar Phys.* **144**, 15.  
 Wilson, P. R., McIntosh, P. A., and Snodgrass, H. B.: 1990, *Solar Phys.* **127**, 1.

- Wolfson, R. L. T.: 1982, *Astrophys. J.* **255**, 774.  
Wolfson, R. L. T.: 1995, *Astrophys. J.* **443**, 810.  
Wolfson, R. and Low, B. C.: 1992, *Astrophys. J.* **391**, 353.  
Wolfson, R., Conover, C., and Illing, R. M. E.: 1987, *J. Geophys. Res.* **92**, 13 641.  
Woltjer, L.: 1958, *Proc. Nat. Acad. Sci.* **44**, 489.  
Wu, S. T., Guo, W. P., and Wang, J. F.: 1995, *Solar Phys.* **157**, 325.  
Zirin, H.: 1983, *Astrophys. J.* **274**, 900.  
Zirin, H.: 1985, *Astrophys. J.* **291**, 858.  
Zirin, H.: 1988, *Solar Astrophysics*, Cambridge University Press, Cambridge.  
Zirker, J. B. (ed.): 1977, *Coronal Holes and High-Speed Wind Streams*, Colorado Associated Universities Press, Boulder.  
Zirker, J. B.: 1993, *Solar Phys.* **148**, 43.